Theses and Dissertations--Civil Engineering   Civil Engineering

2024

GEOPHYSICAL METHOD USED FOR THE DETERMINATION AND PREDICTION OF SOIL STRENGTH AND STIFFNESS PARAMETERS

Dabo Adama

University of Kentucky, dad230@uky.edu

Author ORCID Identifier:

https://orcid.org/0009-0006-0211-0811

Digital Object Identifier: https://doi.org/10.13023/etd.2024.168

Right click to open a feedback form in a new tab to let us know how this document benefits you.

STUDENT AGREEMENT:

I represent that my thesis or dissertation and abstract are my original work. Proper attribution has been given to all outside sources. I understand that I am solely responsible for obtaining any needed copyright permissions. I have obtained needed written permission statement(s) from the owner(s) of each third-party copyrighted matter to be included in my work, allowing electronic distribution (if such use is not permitted by the fair use doctrine) which will be submitted to UKnowledge as Additional File.

I hereby grant to The University of Kentucky and its agents the irrevocable, non-exclusive, and royalty-free license to archive and make accessible my work in whole or in part in all forms of media, now or hereafter known. I agree that the document mentioned above may be made available immediately for worldwide access unless an embargo applies.

I retain all other ownership rights to the copyright of my work. I also retain the right to use in future works (such as articles or books) all or part of my work. I understand that I am free to register the copyright to my work.

REVIEW, APPROVAL AND ACCEPTANCE

The document mentioned above has been reviewed and accepted by the student's advisor, on behalf of the advisory committee, and by the Director of Graduate Studies (DGS), on behalf of the program; we verify that this is the final, approved version of the student's thesis including all changes required by the advisory committee. The undersigned agree to abide by the statements above.

<div align="right">

Dabo Adama, Student

Dr. L. Sebastian Bryson, Major Professor

Dr. Mei Chen, Director of Graduate Studies

</div>

GEOPHYSICAL METHOD USED FOR THE
DETERMINATION AND PREDICTION OF SOIL STRENGTH
AND STIFNESS PARAMETERS

_____

THESIS
_____

A thesis submitted in partial fulfillment of the
requirements for the degree of Master of Science in the
College of Engineering
at the University of Kentucky

By

Dabo Adama

Lexington, Kentucky

Director: Dr. L. Sebastian Bryson, Professor of Civil Engineering

Lexington, Kentucky

2024

ABSTRACT OF THESIS

GEOPHYSICAL METHOD USED FOR THE
DETERMINATION AND PREDICTION OF SOIL STRENGTH
AND STIFNESS PARAMETERS

This paper presents the results of an effort to use geophysical measurements such as seismic wave velocities and electrical resistivities to calculate airfield design parameters. The study converts all geophysical measurements to equivalent California Bearing Ratio (CBR) values, comparing CBR values estimated from DCP penetration resistance with CBR values estimated from shear wave velocity and electrical resistivity values. Relationships linking the geophysical measurements to CBR estimates were established using laboratory data and applied to field in-situ measurements. The elastic modulus (E) is the stiffness parameter involved in predicting soil strength and stiffness. This research aims to relate electrical conductivity and modulus by using a box test.

A sigmoidal model was proposed for the prediction of elastic modulus as a function of conductivity, which performed well with high-strength soil. Soil tests from two different source locations were considered at different moisture contents, with a total of eight tests analyzed. The results show that elastic modulus values estimated from both shear wave velocity and DCP measurements tend to perform better at low conductivity and higher stiffness soil types. However, the elastic modulus from the proposed model does not match well with the DCP or shear wave velocity data when applied a field site located in Rouen, France. Overall, this study demonstrates the viability of using geophysical methods to assess airfield suitability and improve the accuracy of soil assessment in airfield design.

KEYWORDS: Seismic Wave, CBR, Electrical conductivity/resistivity, Modulus, Soil properties

Dabo Adama
_____

04/25/2024
_____
Date

GEOPHYSICAL METHOD USED FOR THE
DETERMINATION AND PREDICTION OF SOIL STRENGTH
AND STIFNESS PARAMETERS

By
Dabo Adama

| L. Sebastian Bryson |
| Director of Thesis |

| Mei Chen |
| Director of Graduate Studies |

| 04/25/2024 |
| Date |

To *my wife Toure Soumare, my mum Cisse Soumare, my brothers and sisters, this work is dedicated to.*

ACKNOWLEDGMENTS

TABLE OF CONTENTS

LIST OF TABLES

LIST OF FIGURES

CHAPTER 1. INTRODUCTION

1.1 PROBLEM STATEMENT

It is necessary to conduct an accurate assessment of the subgrade stability prior to the construction of a new airfield in semi-prepared terrain or the repair of an existing airfield. The shear strength of the subgrade soil is a measurement of stability that also describes the load-carrying capacity of the soil. Failure of the soil support system beneath airfields can be caused by insufficient soil subgrade strength, resulting in catastrophic damage to aircraft and ground equipment.

Determining geotechnical soil parameters involved in the stability of airfield is expensive and time-consuming. Properties such as elastic modulus, and soil strength, involve laboratory tests that are limited in feasibility. Traditional laboratory tests only provide discrete data at a certain condition, time, or place. The use of electrical data measurements has the capability to help determine soil related properties such as porosity, moisture content, stiffness, and strength (Hurley, 2021).

Soil characteristics have been noted to directly affect not only the geophysical behavior of a subgrade soil system but also the stiffness and strength of the soil system. They include soil type, stress history, degree of saturation, pore structure, and current stress state. These characteristics also affect the strength and deformation (stiffness) behavior of a soil system. Therefore, geophysical measurements in soils will likely give a reliable estimate subgrade engineering behavior.

The geophysical behavior of a subgrade soil system is directly affected by characteristics such as soil type, pore structure, degree of saturation, stress history, and current state of stress. These characteristics also affect the strength and deformation (stiffness) behavior of a soil system. Therefore, geophysical measurements in soils will likely give a reliable estimate subgrade engineering behavior. Geophysical techniques not only give a more natural (rather than just an empirical) relationship for modulus, but they also provide spatial data over sites of interest, as compared to DCP measurements which provide data at discrete locations and at discrete depths.

The relationship between CBR penetration, strength, and stiffness, determined both in the laboratory and the field, has been the subject of extensive research (Narzary and

Ahamad, 2018; (Mendoza and Caicedo, 2019). This study uses geophysical measurements like seismic wave velocities and electrical resistivities to calculate airfield design parameters. It compares CBR values from DCP penetration resistance with CBR values from shear wave velocity and electrical resistivity. Relationships between geophysical measurements and CBR estimates are established using laboratory data.

These relationships are then applied to field in-situ measurements, which are used to calculate airfield design parameters like prepared layer thickness, allowable load, and aircraft pass number. The results show that CBR and modulus values from shear wave velocity measurements match DCP-derived CBR and modulus values, demonstrating the viability of using geophysical methods to assess airfield suitability.

1.2   OBJECTIVES

The study suggests using geophysical techniques and methods to predict soil strength and stiffness parameters influenced by geotechnical and temporal application: This research uses geophysical measurements like seismic wave velocities and electrical resistivities to calculate airfield design parameters. It converts all geophysical measurements to equivalent CBR values, comparing CBR values from DCP penetration resistance with shear wave velocity and electrical resistivity values. Relationships between geophysical measurements and CBR estimates are established using laboratory data and applied to field in-situ measurements. Results show that shear wave velocity measurements match DCP-derived CBR values, proving the viability of using geophysical methods for airfield suitability assessment.

This investigation proposes a new approach to relating laboratory box tests to field conditions using geophysical measurements like seismic wave velocities and elastic conductivities. It demonstrates the link between elastic moduli estimated from shear wave velocity and DCP as a function of electrical conductivity. The geophysical methods used in the box test help determine unsaturated parameters and soil behavior, as field conditions cannot be controlled.

1.3   CONTENTS OF THESIS

Chapter 1: Introduction section including problem statement and objectives of this thesis.
Chapter 2-3: Paper published and to be submitted with the contents verbatim.
Chapter 2: The building of new airfields on semi-prepared terrain and the maintenance and repair of existing airfield requires a quick and accurate assessment of the subgrade soil strength and stability. Failure of the soil support system beneath airfields can be caused by insufficient soil subgrade strength, resulting in catastrophic damage to aircraft and ground equipment.

The suitability of an airfield for regular operations is a function of the stiffness of the subgrade soil under small deflections. Stiffness is the tendency of a soil to deform under load at small strain values. Stiffness is characterized by the elastic modulus of the soil. In-situ soil modulus values are commonly estimated from California Bearing Ratio (CBR) values via an empirical relationship.

Currently, the dynamic cone penetration (DCP) method is a technique that is the most widespread option for determining the in-situ CBR. For airfield suitability assessment and design, the DCP penetration resistance is used to estimate an equivalent CBR values from empirical relationships. Therefore, for airfield design, a DCP value is used to estimate a CBR value, which in turn, is used to estimate a modulus value. When these individual empirical equations are combined, the errors inherent to each empirical equation increase by an order of three. Geophysical measurements such as seismic wave velocity can directly quantify modulus and eliminate the need for a multistep empirical process.

This research presents the results of an effort to use geophysical measurements such as seismic wave velocities and electrical resistivities to calculate airfield design parameters. Given that the CBR values are the current standard for airfield suitability assessment and design, this study converted all geophysical measurements to equivalent CBR values. This paper compared CBR values estimated from DCP penetration resistance with CBR values estimated from shear wave velocity and electrical resistivity values. Relationships linking the geophysical measurements to CBR estimates were established using laboratory data. These relationships were then applied to field in-situ measurements. The field in-situ measurements were further used to calculate airfield design parameters

such as prepared layer thickness, allowable load, and the number of aircraft passes. The results of this study show that CBR values estimated from shear wave velocity measurements well matched DCP-derived CBR values. Thus, establishing the viability of utilizing geophysical methods to assess airfield suitability.

Adama, D., Bryson, L. S., and Wang, A. (2023). Airfield suitability assessment from geophysical methods. Transportation Geotechnics, 42, 101059 (ACCEPTED)

Chapter 3: Soil elastic measurements are dependent upon soil state conditions (density and moisture content) and soil stress (effectiveness and stress history). These factors also greatly affect the strength and stiffness responses of soils. Therefore, it is postulated that elastic parameters such as modulus will provide reasonable estimates of soil strength and stiffness. It is also acknowledged that electrical field surveys provide spatial data using relatively non-intrusive methods. The implication is that field electrical data has the potential to provide spatial strength and stiffness data without the need for time-consuming boring and sampling.

In this study, the stiffness parameter involved in predicting is the elastic modulus (E); therefore, this property is being used as the stiffness property of interest. The elastic modulus measures an object or substance's resistance to being deformed elastically when stress is applied to it. Several studies have tried to correlate CBR with the elastic properties of soil since they are linked. More recently, these studies have been extended to develop relationships with other measures of strength and stiffness, such as the elastic modulus, which is the stiffness property of interest in this research.

This research sought to relate electrical conductivity and modulus by using a box test. A sigmoidal model was proposed for the prediction of elastic modulus as a function of conductivity, and it performed well with high-strength soil. Soil from two different source locations was considered at different moisture contents, with a total of eight tests analyzed. The testing includes soil tests from the Kentucky River and Hamburg. The Kentucky River is from the north of Kentucky, near Louisville (Kentucky), while the Hamburg Clay is from Lexington, Kentucky. In this current study, 2 and 3 sets of sensors and accelerometers were installed at different depths. These sensors and accelerometers were placed in the box for 24 hours for equilibrium to be achieved. The sets of 2 and 3

sensors and accelerometers were used for Kentucky River Sand and Hamburg Clay, respectively.

The sensors measured the volumetric water content, electrical conductivity, and matric suction, whereas the accelerometers measured the seismic P and S wave velocities at different depths. This research presents the results of an effort to relate seismic wave velocity and DCP-derived elastic modulus as a function of electrical conductivity to determine the stiffness of soil. For the reported study, elastic modulus values estimated from DCP penetration resistance were compared to equivalent elastic modulus values estimated from shear wave velocity values. These relationships were then used to create a sigmoidal model to relate the stiffness of soil in an unsaturated condition as a function of electrical conductivity.

Relationships linking the geophysical measurements to elastic modulus estimates were established using laboratory data using the Box test. These relationships were then applied to field in-situ measurements. The results of this study show that elastic modulus values estimated from both shear wave velocity and DCP measurements tend to perform better at low conductivity and higher stiffness soil types. The results of this study show that elastic values estimated from shear wave velocity measurements trend well with DCP-derived elastic modulus values. On the contrary, the elastic modulus from the proposed model does not match well with the DCP or shear wave velocity data when applied on the French site.

Adama, D., and Bryson, L. S. (2024). Determination of Soil Stiffness Parameters using Electrical Conductivity and Shear Wave velocity Measurements from Laboratory Scale Testing. Applied Geophysics. (TO BE SUBMITTED).

Chapter 4 presents the conclusions section that summarizes the findings from this research.

Appendix A presents the geophysical   and geotechnical data variation with depth at area A2.

Appendix B presents the CBR and modulus data from the box test.

CHAPTER 2. AIRFIELD SUITABILITY ASSESSMENT FROM GEOPHYSICAL METHOD

2.1 INTRODUCTION

It is necessary to conduct an accurate assessment of the subgrade stability prior to the construction of a new airfield in semi-prepared terrain or the repair of an existing airfield. The shear strength of the subgrade soil is a measurement of stability that also describes the load-carrying capacity of the soil. Failure of the soil support system beneath airfields can be caused by insufficient soil subgrade strength, resulting in catastrophic damage to aircraft and ground equipment. The California Bearing Ratio (CBR) value is an index that is used to evaluate the strength of the subgrade soil in pavement and airfield design applications. The CBR value is an index that is used to evaluate the strength of the subgrade soil in airfield construction. The CBR is the ratio of the penetration resistance of a subgrade soil to the penetration resistance in a specimen of a standard crushed stone base material.

Current Mechanistic-Empirical (M-E) pavement design principles used to design highways and airfield pavements realize that elastic pavement design is not driven exclusively by the strength of unbound pavement materials, but by their stiffness under small deflections. Stiffness is the tendency of a soil to deform under load at small strain values. In terms of stress and strain, stiffness is characterized by the elastic modulus of the soil. The elastic modulus of the in-situ subgrade soil is often estimated from the CBR values using empirical relations.

Currently, the dynamic cone penetration (DCP) method is a technique that is the most widespread option for determining the in-situ CBR. Field subgrade CBR values are estimated using DCP-derived empirical relationships. When combined, the inherent errors associated with each empirical equation (i.e., DCP-to-CBR and CBR-to-Modulus) are compounded. Geophysical measurements such as seismic wave velocity can directly quantify modulus and eliminate the need for a multistep empirical process.

The geophysical behavior of a subgrade soil system is directly affected by characteristics such as soil type, pore structure, degree of saturation, stress history, and current state of stress. These characteristics also affect the strength and deformation

(stiffness) behavior of a soil system. Therefore, geophysical measurements in soils will likely give a reliable estimate subgrade engineering behavior. Geophysical techniques not only give a more natural (rather than just an empirical) relationship for modulus, but they also provide spatial data over sites of interest, as compared to DCP measurements which provide data at discrete locations and at discrete depths.

The relationship between CBR penetration, strength, and stiffness, determined both in the laboratory and the field, has been the subject of extensive research (Narzary and Ahamad, 2018; (Mendoza and Caicedo, 2019) . The elastic modulus of the soil, which characterizes stiffness, is taken as the initial tangent modulus (Rahardjo et al., 2011); (Kim et al., 2019) .The modulus has been correlated with the CBR values in a number of studies. The strength of subgrade materials and pavement layers has been assessed using the correlation between CBR and Dynamic Cone Penetrometer (DCP).

In the recent investigation, an attempt has been made to develop relationships that can be used to estimate subgrade soil strength in terms of elastic modulus and CBR values using in-situ test results of Dynamic Cone penetrometer (Mukabi 2016; Bryson and Sayre 2021; Kang et al., 2022). To analyze possible unimproved landing zones, geophysical parameter such as electrical resistivity and seismic wave velocities were used to determine strength and stiffness properties and their relationship with DCP penetration resistance(Mayne and Rix, 1995). Several researchers (Cheng et 2011; Muttashar and Bryson 2020; Bryson and Sayre 2021) have made a connection between the shear wave velocities measurement and strength parameters such as undrained shear strength and phi angle. The CBR is a penetration test similar to a small strain bearing capacity test. Thus, the premise is shear wave velocity measurement can be used to determine CBR.

Although the CBR is not a measure of shear strength, it can be considered a shear strength index. Crawford and Bryson (2018) showed that there is a link between electrical measurements and shear strength characteristics under drained conditions therefore this study aims to combine various techniques to develop a methodology that connects electrical measurements and shear strength. Other investigations (Wang et al., 2016; Adebisi et al., 2016) demonstrate a correlation between CBR and electrical resistivity. Thus, the premise of this research is that CBR may be used to estimate strength by using

electrical measurements. Other studies shows that good correlation between geophysical electric method and other geotechnical characteristics to predict CBR (Bery, 2016).

This paper presents the results of an effort to use geophysical measurements such as seismic wave velocities and electrical resistivities to calculate airfield design parameters. This paper compared CBR values estimated from DCP penetration resistance with CBR values estimated from shear wave velocity and electrical resistivity values. Relationships linking the geophysical measurements to CBR estimates were established using laboratory data. These relationships were then applied to field in-situ measurements. The field in-situ measurements were further used to calculate airfield design parameters such as prepared layer thickness, allowable load, and the number of aircraft passes. The results of this study show that CBR values estimated from shear wave velocity measurements well matched DCP-derived CBR values. Thus, establishing the viability of utilizing geophysical methods to assess airfield suitability.

2.2   GENERAL ELASTIC THEORY

The stiffness of a material is defined as a measure of resistance to deformation (Sheriff, 2002) and is ultimately related to the elastic moduli of a material that describes the behavior of the material under stress. Stiffness is defined by two elastic Parameters: the shear modulus, G, and Poisson's ratio, ν. From general elastic theory, the shear modulus is related to the modulus of elasticity, E, via Poisson's ratio (Sheriff and Geldart, 1995) as,

$$E = 2(1+\nu)G \qquad (2\text{-}1)$$

The shear modulus describes the tendency of distortional deformation (i.e., shearing), whereas the modulus of elasticity describes the deformation tendency along the axis of stress. Seismic wave propagation through an elastic material is governed by the moduli and the mass density of the material (Foti et al., 2002). Specifically, the primary elastic parameter can all be written in terms of seismic wave velocities given as,

$$G = \rho V_s^2 \qquad (2\text{-}2)$$

$$\nu = \frac{0.5 \left(\dfrac{V_p}{V_s} \right)^2 - 1}{\left(\dfrac{V_p}{V_s} \right)^2 - 1} \qquad (2\text{-}3)$$

where V_s = the shear wave velocity (often referred in literature as the S-wave velocity); ρ = bulk mass density; V_p = the compressional wave velocity (often referred in literature as the P-wave velocity); In general, deformation includes both axial and distortional changes. Therefore, the most comprehensive definition of stiffness should include both shear and elastic moduli and by extension compression and shear wave velocities. The elastic (i.e., small strain) modulus can be written in terms of compressional and shear velocities as,

$$E = \rho V_s^2 \frac{3 \left(\dfrac{V_p}{V_s} \right)^2 - 4}{\left(\dfrac{V_p}{V_s} \right)^2 - 1} \qquad (2\text{-}4)$$

From the preceding relations, it can be concluded that design methods based on the primary elastic parameter (e.g., airfield in semi-prepared terrain design methodologies) can be developed from independent measures of V_s, V_p, and ρ. In practice, the V_p/V_s ratio varies between 2.5 to 1.5 for near-surface soils with an average of approximately 2.0 (Tatham, 1982; Carvalho et al., 2009). Using the average value of the ratio, allows for reasonable estimates of V_p from measures of V_s alone.

2.3 MEANS AND METHODS

The premise of this study was that elastic parameters that are directly derived from measurements of shear and compressional wave velocities can be used to design the surface of an airfield. The soil test results from the study done by Davich et al. (2004) for the Minnesota Department of Transportation (MNDOT) were used to evaluate this premise. The Davich et al. (2004) study compared shear modulus and resilient modulus

data of several pavement foundation materials to investigate a possible relationship between the two moduli.

2.3.1 Test Soils

The Davich et al. (2004) study used six soil samples that represented a range of granular materials that were used as "selected granular or granular" subbase in pavement structures all over Minnesota. Sample A, Sample D, Sample F, Sample H, Sample J, and Sample N were the names of the soils used in the study. For this current study, the identifying system used by Davich et al. (2004) is used herein so that data generated from this current study can be directly compared to data provided in the Davich et al. (2004) study. For each soil sample, index tests were performed including the grain size distribution, specific gravity, and standard Proctor compaction tests. Table 2-1 shows the results of the index tests for the soils. In the table, "Grav Moist" is the gravimetric moisture content defined as the weight of water in a soil mass divided by the weight of solids in the mass.

It is noted in the table that each soil sample has test data from more than one test. For each sample, these numbers represent moisture and density points along the Proctor curves. The grain sizes distributions of the soil samples are shown in Figure 2-1. The figure shows that the samples included well-graded sand (SW from the Unified Soil Classification System – Samples A, D, and N), poorly-graded sand (SP from the Unified Soil Classification System – Sample J), and silty sand (SP-SM and SM from the Unified Soil Classification System – Samples F and H).

Table 2-1 Index test data for the test soils (data from Davich et al. 2004).

Test #	Sample	Grav Moist (%)	Bulk Density (kg/m^3)	Dry Density (kg/m^3)	Specific Gravity	Porosity	Degree of Saturation
Test #2	(A)	3.4	2189	2117	2.68	0.208	0.348
Test #4	(A)	5.3	2283	2168	2.68	0.189	0.611
Test #6	(A)	7.6	2394	2225	2.68	0.167	1.000
Test #8	(D)	2.7	2007	1954	2.68	0.269	0.197

Test #10	(D)	6.1	2105	1984	2.68	0.257	0.471
Test #14	(F)	3.4	1890	1828	2.68	0.316	0.197
Test #15	(F)	5.7	1945	1840	2.68	0.311	0.338
Test #16	(F)	6.3	1974	1857	2.68	0.305	0.385
Test #17	(F)	9	2054	1884	2.68	0.295	0.577
Test #18	(F)	7.3	1988	1853	2.68	0.307	0.443
Test #20	(H)	3.5	1793	1732	2.68	0.352	0.173
Test #21	(H)	7.4	1890	1760	2.68	0.341	0.383
Test #22	(H)	7.1	1885	1760	2.68	0.341	0.367
Test #23	(H)	11	1982	1786	2.68	0.332	0.594
Test #24	(H)	10.6	1978	1788	2.68	0.331	0.575
Test #26	(J)	3.5	1914	1849	2.68	0.308	0.211
Test #28	(J)	5.9	1968	1858	2.68	0.305	0.361
Test #30	(J)	8.6	2013	1854	2.68	0.306	0.522
Test #32	(N)	3.1	2001	1941	2.68	0.274	0.221
Test #34	(N)	5.5	2152	2040	2.68	0.237	0.476
Test #36	(N)	7.9	2227	2064	2.68	0.228	0.719
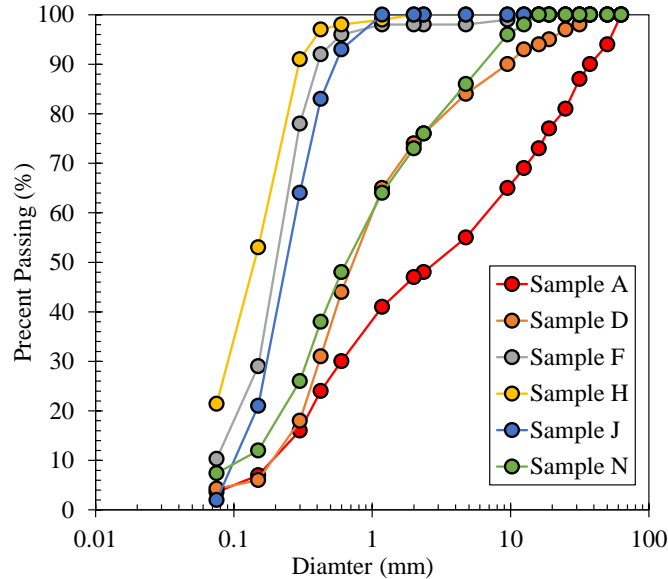
Figure 2-1 Grain size distribution of the test soils.

2.3.2 Seismic Wave Testing

Bender elements (BE) were installed in a standard triaxial cell and used to measure the compressional and shear wave velocities. The triaxial specimens had an average diameter of 152 mm and a length of approximately 305 mm. Davich et al. (2004) reported that particles larger than 13 mm were removed from the samples to minimize the effects of bulk density variations on wave velocity measurements. The shear wave velocities of the samples were measured using the GDS-BES system (GDS Instruments Ltd., Hook, United Kingdom) composed of bender elements inserted to the top cap and the pedestal of the triaxial cell. Bender elements are piezoelectric elements cantilever strips that are in direct contact with the soil sample. Motion in the benders is induced by sending an electrical pulse to one of the elements. The wave produced by the element propagates through the specimen and induces a voltage in a second bender element located on an opposing surface.

Shear waves are generated by motion perpendicular to the axis of the sample and compression waves are generated by motion parallel to the axis of the sample. Davich et al. (2004) used a series of 2 MHz to 5 MHz wave pulses as input signals for the benders. The wave travel times were found using the cross-correlation method, which

Davich et al. (2004) reported were obtained from GDS automated Bender Elements Analysis Tool (BEAT) software. The wave velocities were obtained for each sample once the confining stress was applied, at the beginning of the loading phase of testing. Figure 2-2 shows the shear wave velocities that were measured for each of the samples. The velocity of the shear waves is shown as a function of the confinement pressure. Figure 2-2 shows the shear wave velocities data from the samples plotted as a function of the confining pressure.
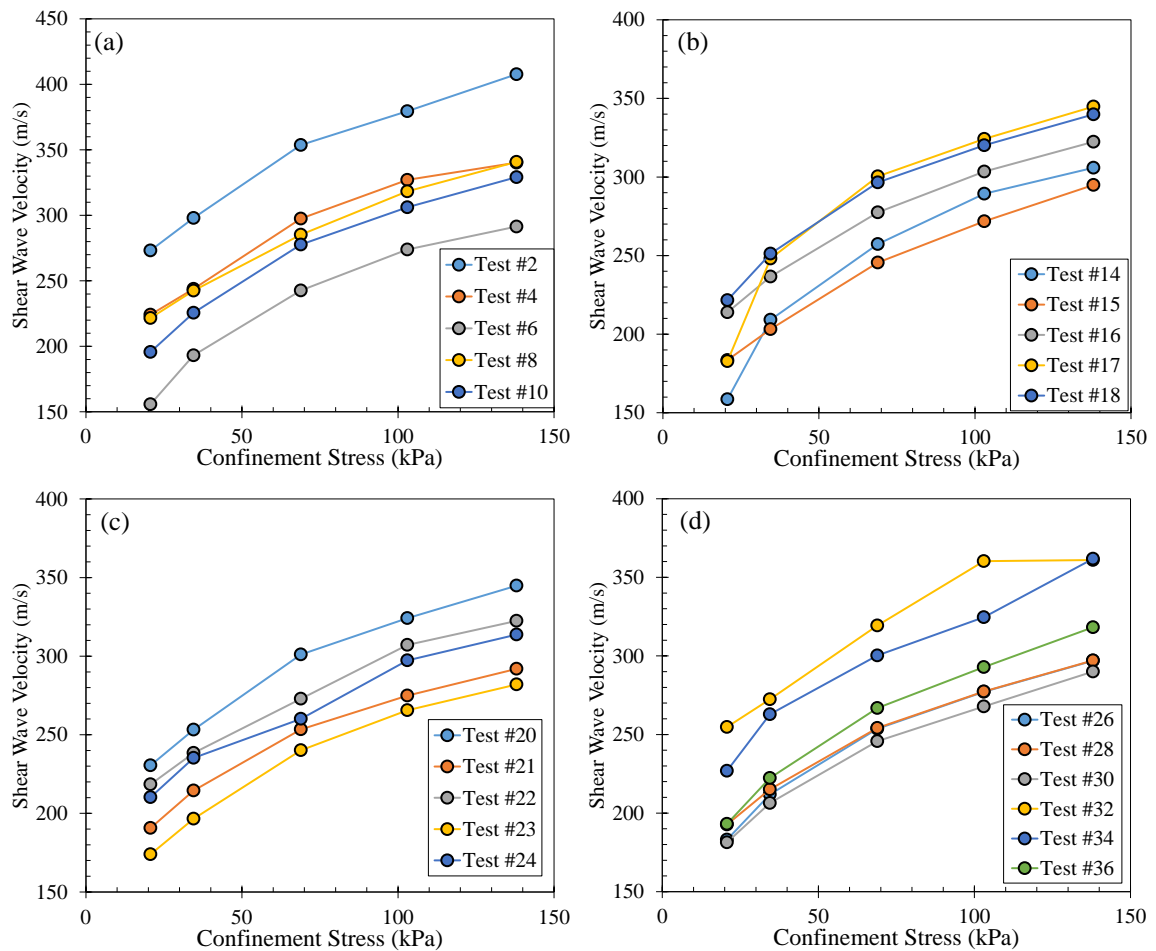
Figure 2-2 Shear wave velocity measurements as functions of the confinement pressure: (a) Sample A and Sample D; (b) Sample F; (c) Sample H; (d) Sample J and Sample N.

Aside from the data showing the wave velocities varied according to confining pressure, material and moisture dependencies were not easily discerned. Typically, shear wave velocities are considered seismic characteristics. However, these are influenced strongly by confining stresses, pore pressures, fluid saturations, temperature, and porosity, to name

only a few. This contribution focuses on how these different factors interact to result in a shear wave velocity observed.

Figure 2-3 shows the compression wave data from the samples plotted as a function of confining pressure. It must be remembered that the data reflects Proctor measurements in which the volume of solids is not constant between each point. Consequently, the porosities and the degree of saturation are not constant for a given soil. Regardless, Figure 2-3 does present the data as measured.
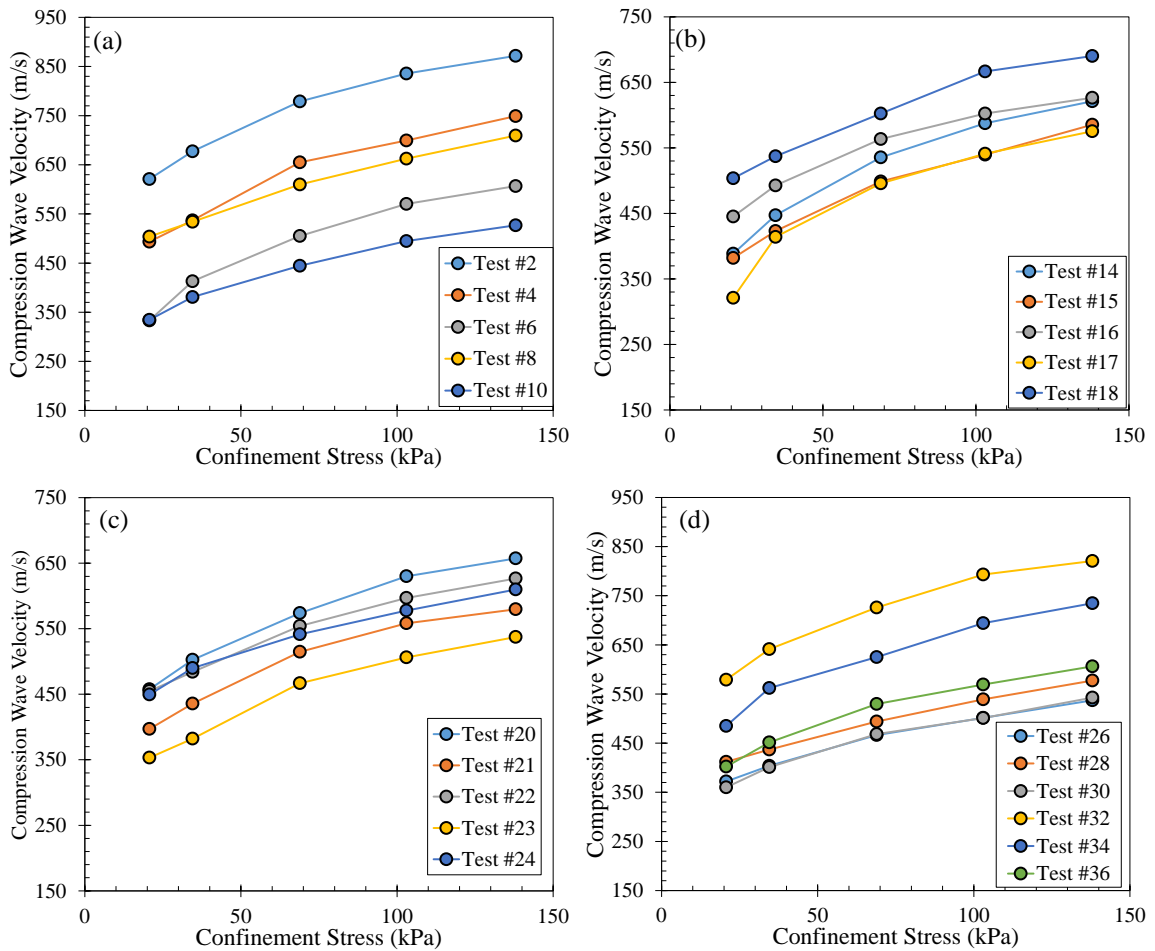
Figure 2-3 Compression wave velocity measurements as functions of the confinement pressure: (a) Sample A and Sample D; (b) Sample F; (c) Sample H; (d) Sample J and Sample N.

2.4   DATA ANALYSIS

As observed from Equation 2-4, the modulus of elasticity was calculated directly from measures of compressional and shear wave velocities. The relation between the shear

wave velocity and the normalized confinement pressure is best described by a power function (Santamarina and Aloufi, 1999; Santamarina et al., 2001). The shear wave velocities implicitly consider the bulk mass density of the sample and confinement stress under which the test was performed. Therefore, a direct relationship can be developed between the seismic wave velocity data and the modulus parameter that does not explicitly require bulk mass density of confinement pressure. Figure 2-4 presents a basic analysis of elastic modulus as a function of the shear wave velocity.
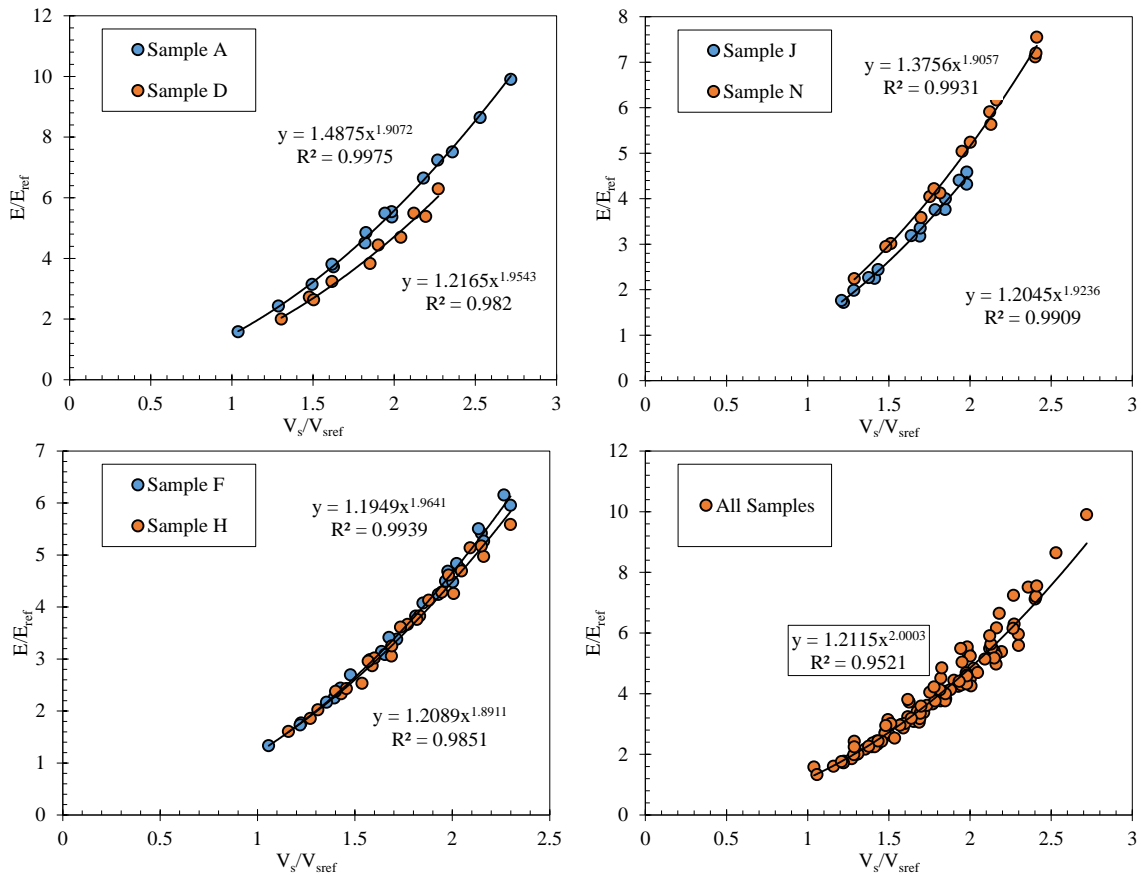
Figure 2-4 Basic analysis of the elastic modulus and shear wave velocity data. (data from Davich et al. 2004).

In Figure 2-4, the measured elastic modulus data are plotted as a function of the measured shear wave velocity data. The elastic modulus values are normalized by a reference elastic modulus, E_{ref} set to 100 MPa. The sole purpose of the reference modulus is to scale the measured modulus values and make the resulting parameter dimensionless. The shear wave velocity values have also been normalized with a reference shear wave

velocity, V_{sref}. For this study, V_{sref} = 150 m/s, which was arbitrarily chosen as a typical value for loose to medium dense sands (Hardin and Richart, 1963).

As dictated by Equation 2-5, the basic relation shown in Figure 2-4 reverts to a power function given as,

$$\frac{E}{E_{ref}} = \beta \left(\frac{V_s}{V_{ref}} \right)^2$$

(2-5)

where β is a term that describes the influence of the mass density and the Poisson's ratio on the changes in the modulus of elasticity,

$$\beta = \left[\frac{\left(V_{ref} \right)^2}{E_{ref}} \right] \rho \left[2 \left(1 + \nu \right) \right]$$

(2-6)

In the absence of compression wave data that is used in conjunction with the shear wave date to obtain Poisson's ratio, and the mass density accompanying shear wave velocity data, the average β is approximatively 1.21. This average value assumes the Poisson's ratio is approximately 0.33 and the average mass density is approximately 2,030 kg/m^3.

2.5   IMPLEMENTATION OF DIRECT MEASURES OF SHEAR WAVE VELOCITY INTO AIRFIELD DESIGN

Implementation of direct measures of shear wave velocity into airfield design was facilitated using the design graphs presented in the Engineering Technical Letter (ETL) 02-19: Airfield Pavement Evaluation Standards and Procedures. ETL 02-19 provides criteria and guidance for the structural evaluation of airfields using conventional evaluation methods. For the purpose of this study, direct measures of shear wave velocity were implemented in the assessment procedures corresponding to semi-prepared (unsurfaced, expedient-surfaced, or aggregate-surfaced) airfields.

Figure 2-5 presents the design charts dictated by ETL 02-19. The original design charts are given in Figure 2-5(a) and 2-5(c). The charts present the CBR index as a function of the number of aircraft passes, for the gross weight of aircraft. The design charts are

specific to a specific design aircraft. For example, the chart presented in Figure 2-5(a) is for a Boeing C-17 Globemaster III, whereas the chart presented in Figure 2-5(c) is for a Lockheed C-130 Hercules. The different charts account for the landing gear configuration, and by extension, the configuration of the stress points applied to the ground surface. In Figure 2-5, the gross weight is the maximum allowable weight during takeoff (i.e., worst-case loading condition). In the figure, the gross weight for each aircraft approximately varies from "empty" (i.e., self-weight only) to fully loaded. Also, in Figure 2-5 the number of aircraft passes refers to a takeoff and landing of an aircraft similar in gross weight to the design aircraft. The number of passes a soil layer can support serves as a measure of the durability of the soil layer. The required number of passes for a given aircraft at a specific gross weight determines the total layer thicknesses of the airfield sublayers. Regardless of whether the surface consists of high-quality aggregate or a well compacted soil surface, the in-place soil strength determines the number of passes.

The ETL 02-19 design charts were slightly modified to present the soil strength index as a function of elastic modulus, as opposed to CBR. Figures 2-5(b) and 2-5(d) show the design charts in terms of elastic modulus. The elastic modulus characterizes the load response of the soil at small elastic strains. The CBR is a bearing capacity response characterized by a penetration resistance. Airfield suitability describes the deformation behavior of a subgrade soil under repeated loading. Therefore, the elastic modulus is better suited for assessing the suitability of an airfield. For this study, the CBR values were converted into elastic modulus values using the empirical equation presented by Powell et al. (1984). The Powell et al. (1984) equation was modified herein as,

$$E\left(MPa\right) = C_1 \times 17.6\left(CBR\right)^{0.64} \qquad (2\text{-}7)$$

where $= C_1$ is a calibration factor to account for variations in testing conditions, such as variations due to depth (i.e., increased lateral restraint), soil types, moisture content, and stress state. As will be discussed in subsequent sections, the calibration factor was determined for this present study by comparing the modulus values obtained from Equation 2-7 to the modulus values obtained directly from field geophysics data. For Figure 2-5, the calibration factor, C_1 equaled approximately 1.0.
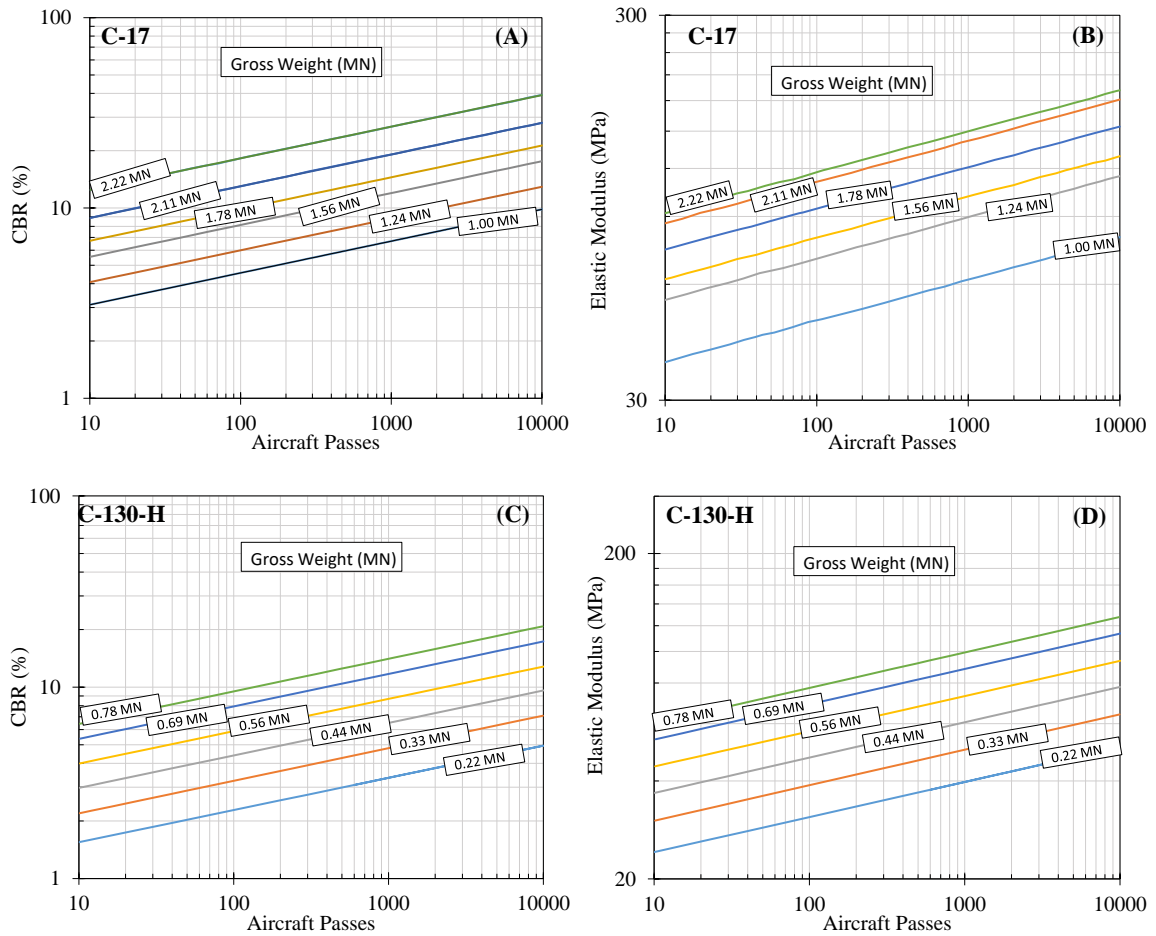
Figure 2-5 Surface soil strength requirements for a typical transport plane on a semi-prepared airfield:(A) C-17 CBR, (B) C-17 Elastic modulus, (C) C-130 H CBR, (D) C-130H Elastic modulus.

Figure 2-5 was expanded to consider any gross weight of aircraft by digitizing the original CBR data from ETL 02-19 and performing a regression analysis. Given that a straight line in a log-log plot yields a power function, the curves in Figure 2-6 can be described generically as,

$$CBR = A\left(P_S\right)^B \tag{2-8}$$

where P_s is number of passes of a particular aircraft, in the case of this research, the C-17 Globemaster and the C-130-Hercules. The A-coefficient is the intercept of a log-log plot and represents the CBR value at one pass, which is the CBR required to support the self-weight of the aircraft. The B-coefficient is the slope of the log-log plot and represents the rate of increase in the number of passes with increasing CBR values. As

seen in Figure 2-6, the assumption is the change in CBR values is proportional to the change in the number of passes. For both the C-17 Globemaster and the C-130-Hercules, the rate of increase was found to be approximately B = 0.17. The A-coefficient is dependent on the gross weight and type of aircraft. Figure 2-6 is a plot of the A-coefficient values for the C-17 Globemaster and the C-130-Hercules.

(A)

(B)
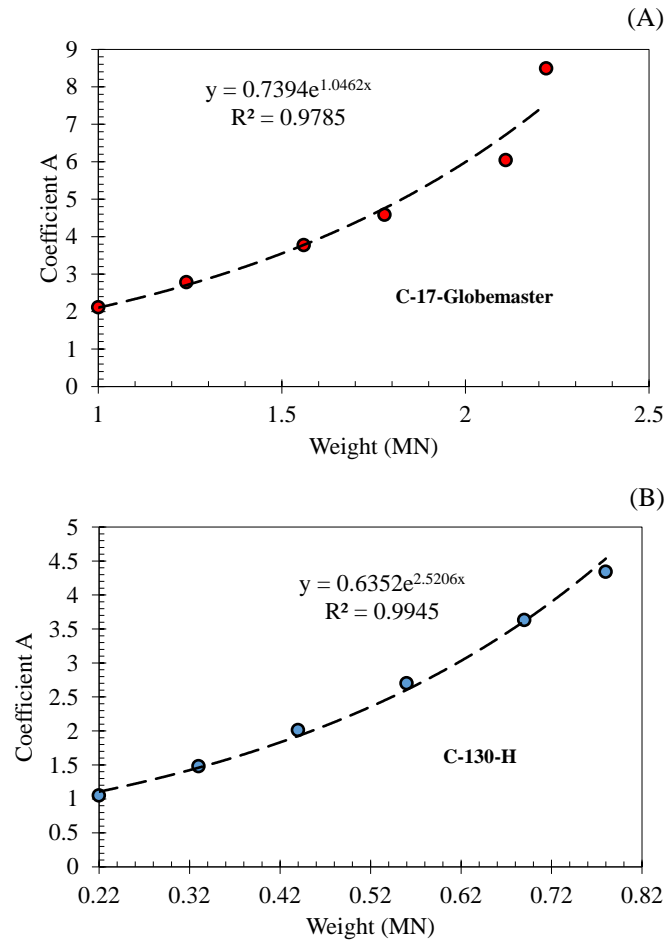
Figure 2-6 The A-coefficient from the regression analysis of the CBR values as a function of gross weight for: (A) C-17-Globemaster aircraft, (B) C-130-H aircraft.

From the regression analysis, a general equation for A-coefficient is expressed as:

$$A = \alpha_1 . \exp(\alpha_2 W_G) \tag{2-9}$$

where α_1 and α_2 are fitting parameters of the regression analysis and are functions of the type of aircraft; W_G is the gross weight of the aircraft in units of MN. Substituting Equation 2-9 into Equation 2-8 produces the expression,

$$CBR = \alpha_1 \cdot \exp\left(\alpha_2 \cdot W_G\right)(P_S)^B \qquad (2\text{-}10)$$

The coefficients for Equation 12 are given in Table 2-2.

Table 2-2 Regression coefficients of the C-17 Globemaster and C-130.

Coefficient	C-17 Aircraft	C-130H Aircraft
α_1	0.7394	0.6352
α_2	1.0462	2.520
B	0.17	0.17

As was discussed previously, shear wave velocity provides a direct measure of the modulus of elasticity. This current study has shown that for small variations of Poisson's ratio and bulk mass density, the elasticity modulus can be determined using Equation 2-7. Therefore, the ETL 02-19 design charts were further modified to show the design requirements of a semi-prepared airfield, in terms of shear wave velocity. Figure 2-7 shows the normalized shear wave velocity as a function of aircraft passes. This version of the design chart allows the suitability of an airfield to be directly determined from field measures of shear wave velocity.
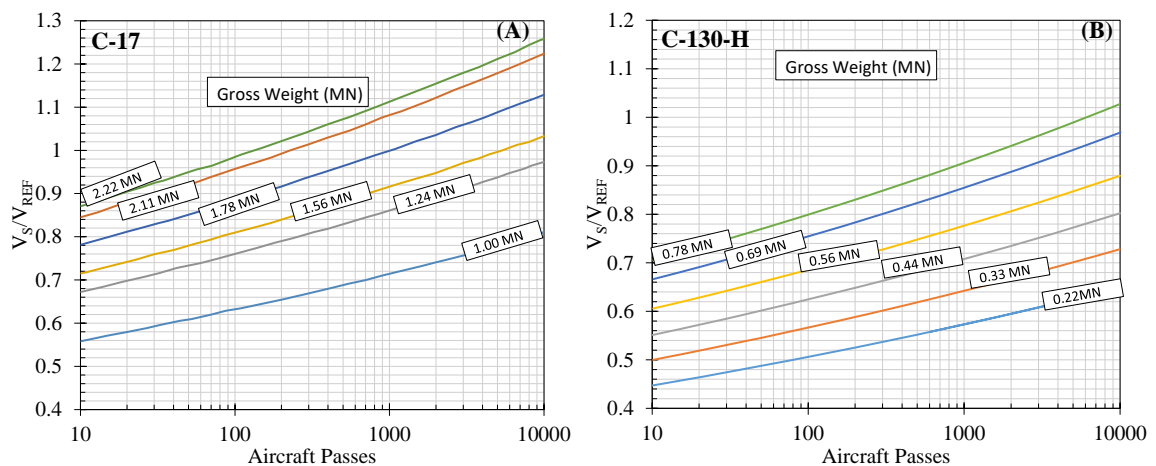
Figure 2-7 Surface soil strength requirements for: (A) a C-17 airframe and (B) C-130-H airframe on a semi-prepared airfield based on shear wave velocity.

20

2.6   FIELD APPLICATION OF SHEAR-WAVE-BASED DESIGN CHART

2.6.1   Field site in France

The efforts proposed herein were focused on developing fundamental geophysical-geotechnical relationships from comprehensive laboratory testing. However, concurrent research efforts are being undertaken by researchers at the University of Rouen Normandy (M2C Lab.), France. The research at the test site located at the CEREMA-Centre for studies on Risks, the Environment, Mobility and Urban planning, in Rouen (France) is focused on relating field electrical, electromagnetic, and seismic geophysical data, to field DCP measurements. To support these efforts, a large-scale test site was developed in which areas of the test site were compacted at targeted CBR strengths. Figure 2-8 shows a section view and plan view of the test site in France.
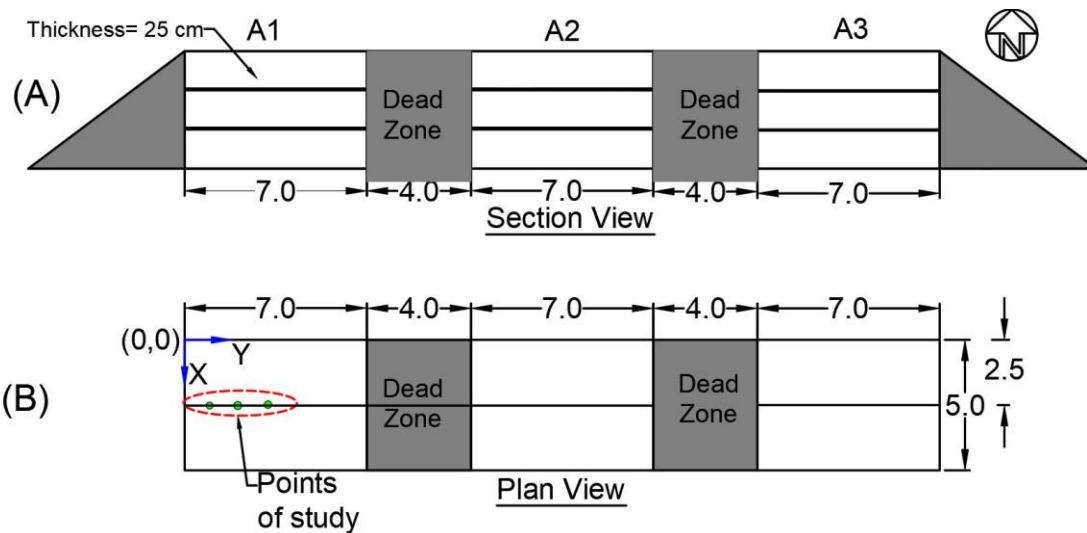
Figure 2-8 Test site. (A) the depth of investigation of the three area, (B) Plan (i.e., arial) view of the three areas of investigation. All dimensions given in the figure are in units of meters.

The test site consisted of three testing areas designated as Area 1 (A1), Area 2 (A2), and Area 3 (A3). Each area is approximately 7 m wide and was constructed in three 250-mm thick compacted soil layers. These areas are separated into 4-m wide "dead zones", so named because it is a region where no reliable data were collected. As seen in Figure 2-8(b), the dimensions of the site are referenced from the origin, located in the northwest corner of the test site. A cartesian coordinate system is assigned to the site in which direct east is assumed to be the Y-direction and direct south is assumed to be the X-direction.

The areas A1, A2, and A3 begin at 0 m, 11.3 m and 22.3 m, respectively and extend to 6.8 m, 17.8 m, and 28.8 m, respectively.

DCP data were collected on a 0.5 m × 0.5 m grid. For the DCP analysis, data were center-averaged along the X-direction. For example, the DCP data at X=2.5 m was an average of DCP data at X=2.0 m, X=2.5 m, and X=3.0 m. The reported data at each location included the position, cumulative depth, number of blows, and depth per blow. Electrical Resistivity (ER) data used for the analysis of the site was the result of an inversion of the raw field ER survey data. For a direct comparison of the electrical data with the DCP data, a profile of the inverted data along the Y-direction was interpolated at the X=2.5 m. Seismic data were obtained from Multichannel Analysis of Surface Waves (MASW) analyses at the site (Using 24 geophones and 25 cm spacing between them). Similar to the ER data, profiles of the seismic data were developed at the locations corresponding to the DCP tests.

2.6.2   Geotechnical and geophysical parameter with variation with depth

The variations of DCP, shear wave velocity, and electrical resistivity data with depth are shown in Figure 2-9. For brevity, Area A1 was considered a characteristic area for the test site. Three points of study were chosen along the centerline of the test site, in the X-direction (i.e., X=2.5 m). The three study points were selected at positions Y=1.3 m, 3.3 m, and 4.3 m (shown previously in Figure 2-9(b). The data obtained from the first 20 cm of the MASW results were unreliable because the errors associated with the dispersion curve fitting for the highest frequencies. At Area 1, the natural ground was located at around 65 cm.
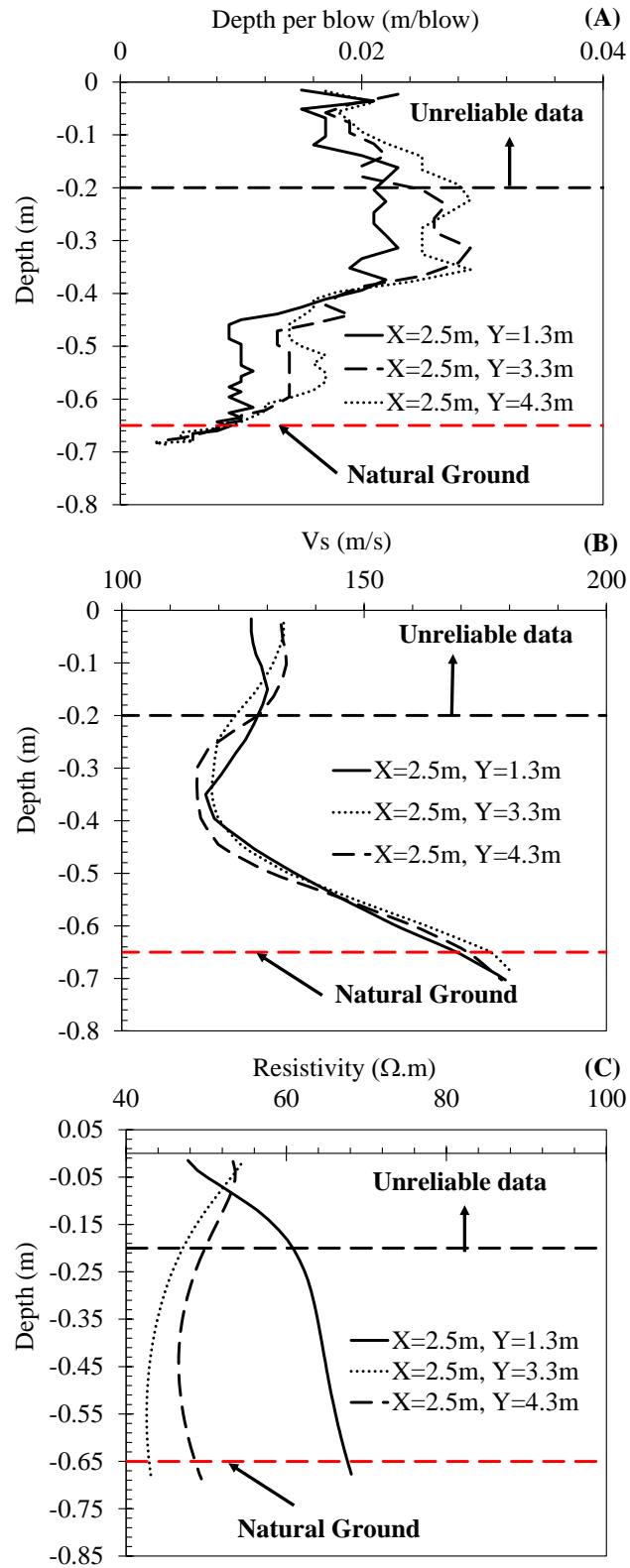
Figure 2-9 Geophysical and geotechnical data variation with depth at Area A1. (A) DCP variation with depth, (B) shear wave velocity variation with depth and (C) electrical resistivity variation with depth.

Figure 2-9(a) shows the DCP variation with depth. The variations at all three points were relatively similar, indicating a consistent compaction effort within Area A1. A maximum depth per blow occurred at an approximate depth of 0.3 m, afterwards the data decreased uniformly with depth. This observation reflects a slightly weaker zone at 0.3 m with an increase in penetration resistance with depth. Although the increase in resistance would tend to imply an increase in strength with depth, when the data are normalized with respect to overburden pressure, the normalized strength remains somewhat constant for the three layers. Figure 2-9(b) shows the shear wave velocity varied between 113 m/s to 180 m/s. The shear wave velocity trends strongly with the DCP data. The shear wave velocity initially increased from the ground surface to a depth of approximately 0.15 m and afterwards decreased from a depth of 0.15 m to 0.38 m.

The decrease in shear wave velocity between 0.3 m and 0.4 m somewhat confirms the DCP data showing a soft zone was in the second layer of Area A1. Figure 2-9(c) shows the variation of electrical resistivity with depth at the three different points which ranging from 42 Ω.m to 89 Ω.m. The electrical resistivity increased with depth at point Y= 1.3m roughly the same rate of increase but decreased with depth at locations Y= 3.3 and 4.3 m from ground surface to a depths of 0.56 m 0.45 m, respectively and increased from theses depths to the natural ground level. As was discussed previously, this similarity is indicative of the uniformity of the test material at the three points of study. It is speculated that the rate of increase and decrease is most likely reflective of the variation in water content with depth, at the time of testing.

2.7 DETERMINATION OF CBR FROM ER, SHEAR WAVE AND DCP AT VARIOUS POINTS OF STUDIES

The CBR value was used as a common variable for comparing the DCP, shear wave velocity, and electrical resistivity data as potential means for assessing the suitability of an airfield. More specifically, all three data were converted to CBR values using empirical equations reported in literature or using empirical equations developed for this research. The DCP method is the most common method used to predict in situ CBR. The CBR data presented in ETL 02-19 was developed using the empirical relationship developed by Webster et al. (1992) and is given as,

$$\log(CBR) = 2.465 - 1.12 \log(DCPI) \tag{2-11}$$

where and DCPI is the penetration resistance or penetration index in units of mm/blow. CBR values estimated from the shear wave velocity data were computed by substituting Equation 2-5 into Equation 2-7. Consequently, CBR is written in terms of shear wave velocity from the following simplified expression:

$$CBR_{VS} = \left[\left(\frac{E_{ref}}{14.545(C_1)} \right) \left(\frac{V_s}{V_{ref}} \right)^2 \right]^{1.5625} \tag{2-12}$$

where CBR_{VS} is the CBR value computed from shear wave velocity.

Laboratory tests were performed to ascertain a relationship between the electrical resistivity and the CBR values. The laboratory tests included CBR tests performed on two silty sand samples (Kentucky River Sand and Ohio River Sand) placed at dry unit weights and gravimetric water contents corresponding to points along the standard Proctor curves for each sample. For the tests, electrical data was measured continuously during the CBR tests using an LCR meter. Specific to the CBR-electrical measurements research, electrical resistivity data were extracted corresponding to the initial state conditions, ER_{in}. Figure 2-10 shows the CBR data as a function of the resistivity.
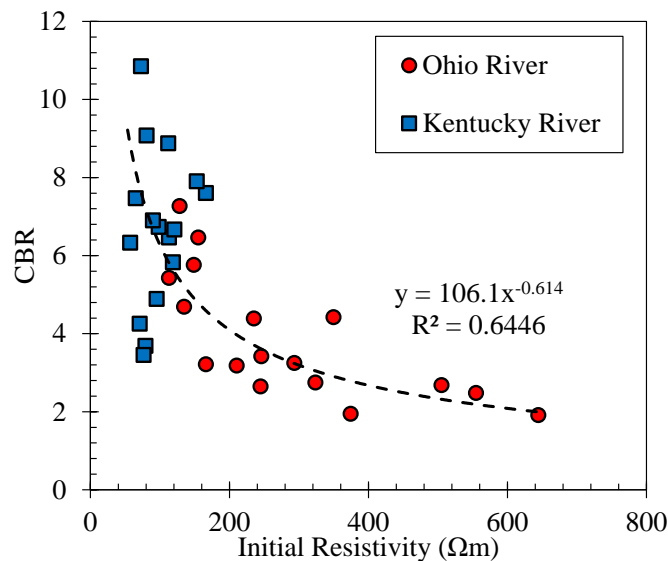
Figure 2-10 Laboratory CBR data as a function on the resistivity measured at the start of CBR penetration.

As shown in Figure 2-10, higher resistivities correspond to lower CBR values. Moreover, Kentucky River Sand data tended to cluster and show relatively minor resistivity variations with changing CBR values. The resistivity or the Kentucky River sand varied between 55.88 to 156.37 $\Omega.m$ compared to the Ohio River sand which had a greater variation of resistivity (107.99 to 525.71 $\Omega.m$) over changes in CBR values. An empirical equation was derived from a regression analysis for the CBR data and the electrical resistivity data given as,

$$CBR_{ER} = 106.1(ER_{in})^{-0.614} \tag{2-13}$$

where CBR_{ER}, is the CBR value determined from the electrical resistivity data and the resistivity data are in units of $\Omega.m$.

Field data shown in Figure 2-9 were input into Equation 2-13 to obtain DCP-derived CBR values, Equation 2-12 to obtain shear wave velocity-derived CBR values, and Equation 2-13 to obtain electrical resistivity-derived CBR values at the Rouen test site, at the three points of study. This comparison of the three equivalent CBR values is shown in Figure 2-11. The C_1 calibration factor for Equation 2-12 was set equal to 1.0 for the Rouen site. As seen in the figure, the CBR values derived from DCP data well matched the CBR values derived from the shear wave velocity data. Both the DCP-derived CBR and the Vs-derived CBR data suggested the presence of a softer zone (i.e., CBR of approximately 8) between 0.3 m and 0.4 m. Although this observation is not definitive of soil behavior in Area A1, it does indicate that shear velocity measurements can perform as well as DCP measurements in determining field CBR values.

The ER-derived CBR values did not match either the DCP-derived CBR values or the Vs-derived CBR values. As is seen in Figure 2-11, The CBR_{ER} data was consistent linear decreasing trend with depth for all three points of study. The preliminary assessment of this observation is that the electrical data was only able to capture the slight variation of the moisture content with depth at the test site and not the variations in the mechanical behavior. Thus, it is recommended that future efforts to relate geophysical electrical methods to mechanical behavior will need to incorporate functions that couple changes in the hydrologic regime with changes in the mechanical behavior.

26
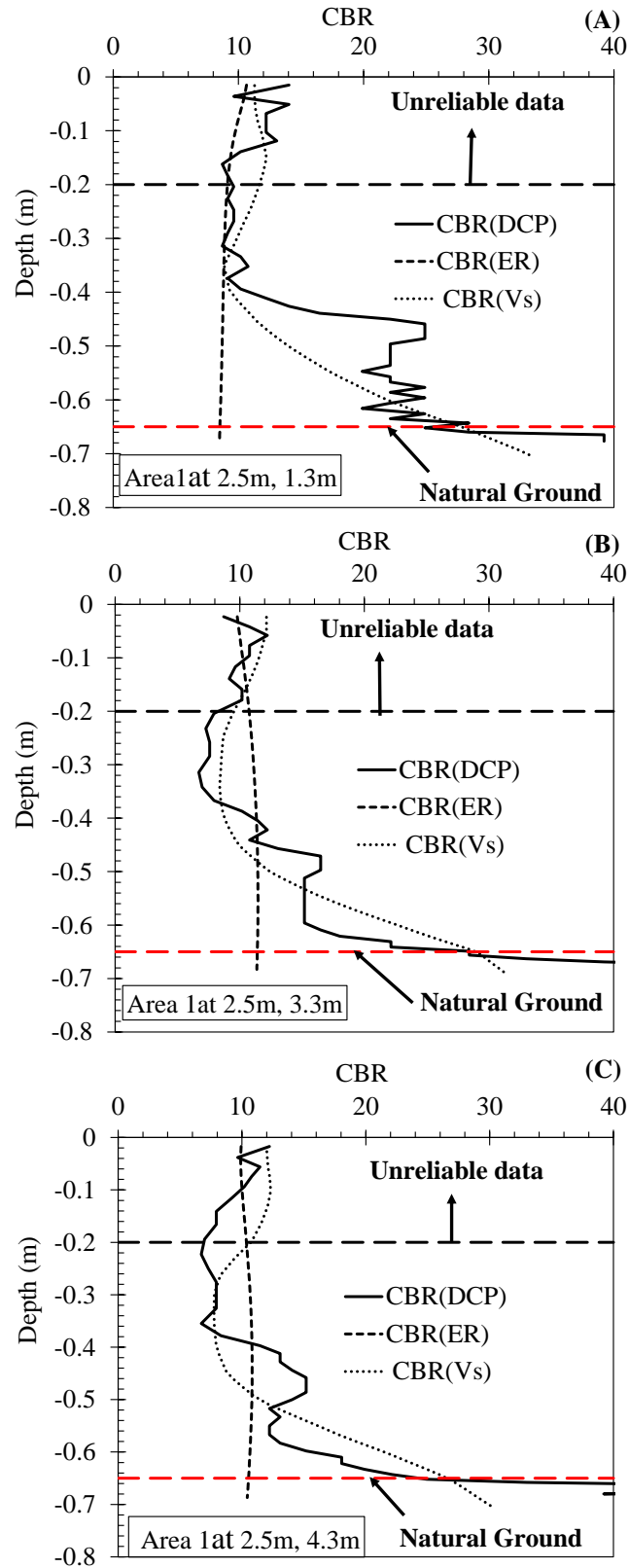
Figure 2-11 CBR based on ERT, DCP, and shear wave velocity and its variation with depth. (A) at 0.3 m, (B) at 0.8 m and (C) at 1.3 m.

2.8 VARIATIONS OF CBR VALUES ALONG A CONSTANT DEPTH OF 0.3 M

Contour maps were generated for the three equivalent CBR data using Surfer 2D Mapping software package from Golden Software. Profile slices were then taken along the Y-direction at the test site to assess the spatial variation of the CBR data. Figure 2-12 displays the three CBR data taken from Area A1 at a constant depth of 0.3 m. The data was obtained from West (Y=0 m) to East (Y=6.8 m). The location of the slice was shown in Figure 2-12(a), 2-12(b), and 2-12(c) and was identified as Line AA'. Similar to CBR variations with depth, Figure 12(d) shows very good spatial agreement with the DCP-derived CBR data and the Vs-derived CBR data. Both data showed the ends of Area A1 as being relatively firm and the middle of Area A1 as less firm. The CBR values ranged from roughly 8.8. to 13 on the West end and ranged from approximately 8 to 14 on the East end.

An observation of the data presented in the figure is that the DCP-derived CBR data showed greater variations of CBR values than the Vs-derived data. However, these variations are most likely due to different data grids used to develop the contours for the two data. The ER-derived CBR data showed an opposite trend from the other two data along the spatial profile. Specifically, the West and East ends of Area A1 were shown to be firmer than the middle. Although the overall magnitude of the ER-derived CBR values were between 7.7 and 11.8 and therefore within the range of the other equivalent CBR values, the ER-derived CBR values lacked spatial variation along the profile. When considering the data in the context of moisture content variations, the ER-derived data appear to indicate that the moisture content was fairly constant along the profile of Area A1, rather than indicating the mechanical behavior was constant.
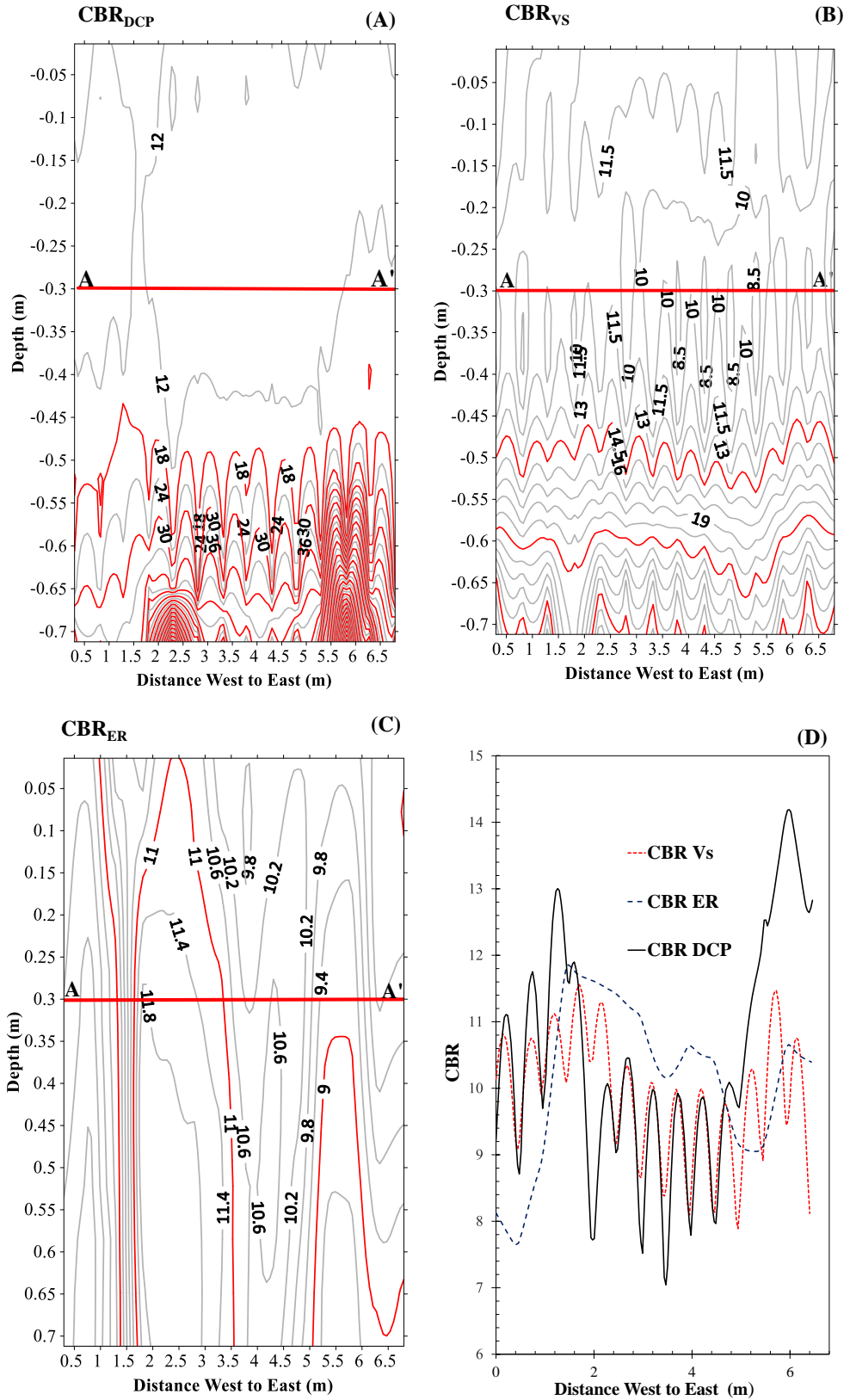
Figure 2-12 CBR values calculated from shear wave velocity, DCP, and ER data at a constant 0.3 m depth across Area 1, going from West-to-East.

2.9 SUITABILITY OF AIRFIELD ASSESSMENT BASED ON THE NUMBER PASSES AND WEIGHT.

The suitability of a potential airfield is assessed based on either the maximum anticipated gross weight of a characteristic aircraft or the number of passes expected for the operational life of the airfield. The maximum anticipated gross weight for a set number of passes can be determined by rewriting Equation 2-10 to solve for gross weight. This yields to following equation:

$$W_G = \left(\frac{1}{\alpha_2}\right) \ln \left(\frac{CBR}{\alpha_1 (P_s)^B}\right) \tag{2-14}$$

Conversely, Equation 2-14 can be rearranged to yield the anticipated number of passes for an assumed gross weight given as,

$$P_S = \left(\frac{CBR}{\alpha_1 \exp(\alpha_2 W_G)}\right)^{\frac{1}{B}} \tag{2-15}$$

The process flow for assessing the suitability of a potential airfield using spatial geophysics data (e.g., shear wave velocity data) rather than discrete data points (i.e., DCP data), requires the user to first use the geophysical data to estimate either the CBR values (i.e., strength index) or directly estimate the elastic modulus values (i.e., stiffness parameter). The spatial strength index values and the spatial stiffness values can be visualized over the potential airfield using contour software. An example of how this process flow can be implemented is given in Figure 2-13. For this example, the C-17 Globemaster was chosen as the characteristic aircraft. For assessing the suitability of the potential airfield based on the number of passes, a weight of 1.56 MN was considered, while 5000 passes were used for assessing the suitability of the potential airfield based on the gross weight.

The assessment criteria for this example were an airfield capable of accommodating either 1000 passes or a maximum gross weight of 1.1 MN. This example used the spatial shear wave velocity data at Area A1 to obtain spatial CBR data. The spatial CBR data were converted to maximum gross weight data using Equation 2-15 and converted to maximum number of passes data using Equation 2-14. These data were subsequently input into the Surfer 2D Mapping software package to facilitate the development of profiles at the Rouen

test site. For brevity, Figure 2-13 presents the West-to-East profile along the centerline of the test site (X=2.5 m), taken at an arbitrary depth of 0.3 m.
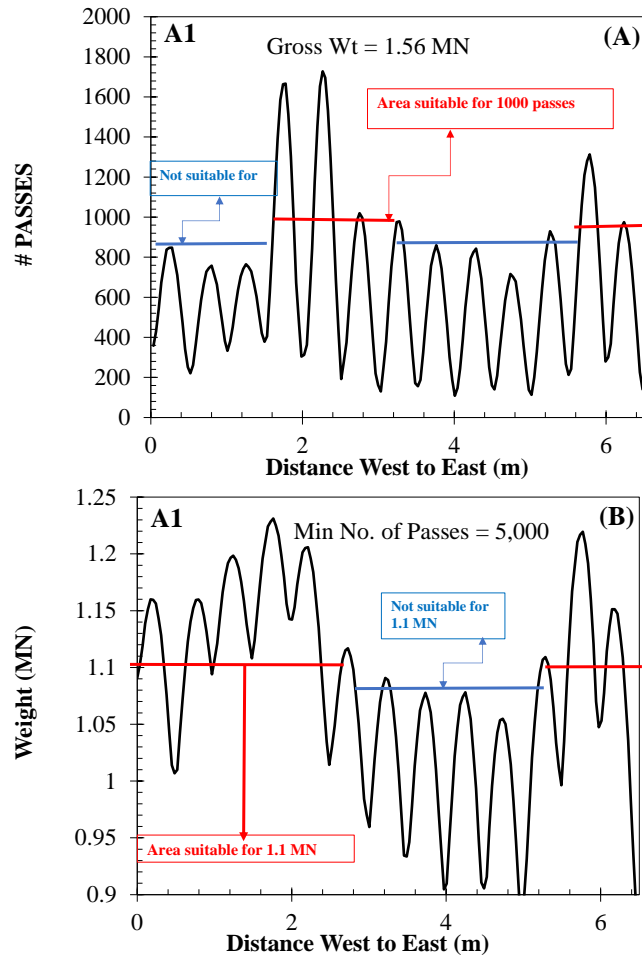
Figure 2-13 Assessment of the suitability of a potential airfield along Area 1 based on: (A) number of passes versus distance (B) weight versus distance.

Figure 2-13(a) presents the locations along Area A1 suitable for 1000 passes, as well as an unsuitable region in which 1000 passes cannot be obtained. Figure 13(b) shows areas that can and cannot support a weight of 1.1 MN. Figure 2-13(a) reveals that the West-to-East distances from 0 m to 1.6 m and 3.4 to 5.6 m are not suitable for the required minimum of 1000 passes. However, West-to-East distances from 1.6 to 3.4 m and the distance beyond 5.6 m meet or exceed the minimum number of passes criteria. As shown in Figure 13(b), the areas that can support 1.1 MN are between 0 and 2.4 m and between 5.2 and 6.5 m, while the areas that are less suitable are between 2.9 and 5.1 m.

CHAPTER 3. DETERMINATION OF SOIL STIFFNESS PARAMETERS USING
ELECTRICAL CONDUCTIVITY AND SHEAR WAVE VELOCITY
MEASUREMENTS FROM LABORATORY SCALE TESTING

3.1   INTRODUCTION

Determining geotechnical soil parameters is expensive and time-consuming. Properties such as elastic modulus, and soil strength, involve laboratory tests that are limited in feasibility. Traditional laboratory tests only provide discrete data at a certain condition, time, or place. The use of electrical data measurements has the capability to help determine soil related properties such as porosity, moisture content, stiffness, and strength (Hurley, 2021). Some study have strongly correlated the a link between geophysical data and soil water characteristic curve by the use of non-destructive electrical resistivity method (Raheem, 2023). Soil characteristics have been noted to directly affect not only the geophysical behavior of a subgrade soil system but also the stiffness and strength of the soil system. They include soil type, stress history, degree of saturation, pore structure, and current stress state.

These characteristics also affect the strength and deformation (stiffness) behavior of a soil system. Therefore, geophysical measurements in soils will likely give a reliable estimate subgrade engineering behavior. According to Santamarina and Aloufi (1999); and Rahardjo et al., (2011), the terms elastic modulus and stiffness are often interchanged. The elastic modulus is defined as the degree of stiffness of an elastic material and is represented as a ratio of stress to strain while stiffness is defined as the tendency of soil to undergo deformation at small load strain values. The elastic modulus is often used for estimation of soil settlement and elastic deformation analysis. For the estimation of elastic deformation and soil settlement analysis, the elastic modulus is used, and it is usually estimated based on correlation with other soil properties, from in-situ or from laboratories. In the labs, triaxial test is used for the estimation though it can also be estimated indirectly using oedometer test. While on the field, Standard Penetration Test (SPT), Cone Penetration Test (CPT), and pressure meter are used.

The elastic modulus values are typically obtained from the California Bearing Ratio (CBR) values by using various empirical relationships (Adama et al., 2023). On the other hand, the empirical relationships from the Dynamic Cone Penetrometer (DCP) are used

for the estimation of field subgrade CBR values. The error from each of these empirical equations (DCP-to-CBR and CBR-to-Modulus) are consequently compounded when they are combined to a final equation. Bryson and Sayre (2021) state that for direct estimation of modulus values, geophysical measurements such as shear wave velocity are employed. Thus, eliminating the need for a multistep process and making this process of determining elastic modulus less costly and time consuming. Because the process of determining elastic properties of soil either by laboratory or in-situ can be time consuming and limited to discrete intervals and feasibility and locations, geophysical measurements such as electrical conductivity and shear wave velocities can provide soil properties such as strength and stiffness at spatial and temporal intervals in less time and effort. Therefore, there is a need to develop a small-scale model in the box tests to describe the variations of the seismic wave and electrical data as a function of stiffness or strength with changes in the unsaturated conditions.

This investigation presents the results of an effort to use geophysical measurements such as seismic wave velocities and electrical conductivities to model a new approach of relating the laboratory box tests to field conditions. For the unsaturated condition in the box test, the geophysical methods used will help determine not only the unsaturated parameters but also the behavior of soil since the condition in the field cannot be controlled and time consuming and labor intensive. In the recent investigations, attempts have been made to develop relationships between elastic moduli strength and stiffness (Yoon and Lee, 2010 Shao et al., 2015; Lee and Yoon, 2015; Cilli and Chapman, 2021; Juarez et al., 2023). Although this research does not directly deal with strength, several study have made linkage between strength and stiffness (Mendoza and Caicedo, 2019). Several researchers have made a connection between elastic moduli and geophysical properties for the construction of an airfield. and the construction of new airfields on semi-prepared terrain and the repair of existing airfield requires a quick and accurate suitability assessment of the subgrade soil strength and stability.

To analyze possible unimproved landing zones, geophysical parameter such as electrical resistivity and seismic wave velocities were used to determine strength and stiffness properties and their relationship with DCP penetration resistance The suitability of an airfield for regular operations is a function of the stiffness of the subgrade soil under

small deflections. This paper presents the results of an effort to use seismic wave velocity and elastic resistivity data to determine airfield design parameters (Bryson and Sayre, 2021; Adama et al., 2023). The elastic modulus of the soil, which characterizes stiffness, is taken as the initial tangent modulus (Rahardjo et al., 2011); (Kim et al., 2019) The modulus has been correlated with the CBR values in a number of studies. The strength of subgrade materials and pavement layers has been assessed using the correlation between CBR and dynamic cone penetrometer (DCP).Other investigation is aimed at establishing a relationship between electrical resistivity and geotechnical parameters such as matric suction and strength (Crawford and Bryson, 2018 ; Abd et al., 2020). Moreover recent findings suggest that resistivity could be used in calculating and predicting moduli for soil (Zhou et al., 2015; Adebisi et al., 2016).

Several researchers (Cheng et 2011; Muttashar and Bryson 2020; Bryson and Sayre 2021) have made a connection between the shear wave velocities measurement and strength parameters such as undrained shear strength and phi angle and stiffness. CBR is a penetration test like a small strain bearing capacity test and describes the mechanical behavior of soil. Thus, the premise is shear wave velocity measurement can be used to determine CBR and elastic modulus since they all describe mechanical behavior of soil and rocks in geotechnical engineering and rock mechanics (Mendoza and Caicedo, 2019).

Recent studies (Lee and Yoon, 2015; Kang and Lee, 2015) have correlated equation between the elastic wave velocity and electrical resistivity. The intent of the box tests is to develop small-scale models to describe the variations of the seismic wave and elastic measurements with changes in the unsaturated conditions. The goal is to develop unique relationships for modulus and elastic modulus values under unsaturated conditions.This research presents the results of an effort to use geophysical measurements such as seismic wave velocities and elastic conductivities to model a new approach of relating the laboratory box tests to field conditions. This paper shows linkage between the elastic moduli estimated from the shear wave velocity and DCP as a function of electrical conductivity. For the unsaturated condition in the box test, the geophysical methods used will help determine not only the unsaturated parameters but also the behavior of soil. Since the condition in the field cannot be controlled, we are using the box test to model the field

conditions. The primary purpose of this research is to determine how the behavior of soil in the box correlates to the behavior of the soil in the field.

3.2   MEANS AND METHODS

The premise of this research in the box test was to elucidate the behavior and activities in the field. This allows us to test several conditions, such as different moisture content, in a controlled manner since we cannot control different conditions in the field. In order to achieve this goal, we conducted our study in a small-scale model of the box tests that can describe how the elastic measurements and seismic wave vary with the unsaturated conditions and change with different moisture content. Two types of soil with four different moisture contents were considered for this research. This study compared the moduli obtained from the shear wave velocity and the DCP data of the Kentucky River Sand and Hamburg Clay to investigate a possible relationship between the modulus of elasticity and the electrical properties of these soils under unsaturated conditions.

3.2.1   Test Soils

This study uses two soil types, ranging from granular material to a fine soil type with different moisture content. Throughout this investigation, soil samples were taken from two different places and evaluated, namely the Kentucky River Sand and the Hamburg Clay. The Kentucky River Sand is naturally occurring coarse sand classified as poorly graded (SP) according to the Unified Classified System (USCS), and the Hamburg Clay is naturally occurring fine-grained soil classified as poorly graded soil (CL) according to the Unified Classified System (USCS). The liquid limit (LL) and the plastic limit (PL) of the Hamburg clay are 33 and 21, respectively. The grain size distributions of the soil samples are shown in Figure 3-1. Moreover, the specific gravity of the Kentucky River Sand and Hamburg Clay is 2.68 and 2.65, respectively.
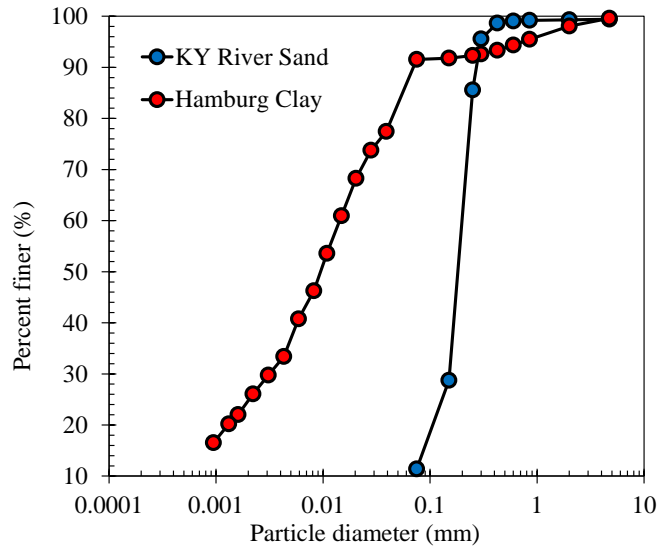
Figure 3-1 Grain size distribution of the test soils.

3.2.2   Moisture and Suction Conditions in the Test Box

Loc A, Loc B, Loc C, Loc D, Loc E, and Loc F Loc G and Loc H were the names of the locations where the moisture content was measured by the sensors in the box test. Loc A to Loc D were the locations where soil moisture content was measured using Kentucky Rivers Sand, whereas Loc E to Loc H were performed on Hamburg Clay. The experiments conducted on the Kentucky River Sand and Hamburg Clay tests were performed in two and three layers, respectively. The accelerometers were double-chained so that three-layer testing could be performed on the Hamburg clay. For each soil sample, we varied the moisture content, including gravimetric water content (the gravimetric moisture content is defined as the weight of water in a soil mass divided by the weight of solids in the mass).

In the tables, "KYS" and "HBC" are used to refer to the Kentucky River Sand and Hamburg Clay, respectively. Moreover, the numbers attached to KYS and HBC refer to the layer in which the measurement of moisture content was estimated for each soil type. Table 3-1 presents the testing conditions such as moisture, density, and degree of saturation and matric suction measured at each layer in the box test. For each sample, these numbers represent moisture points along the Proctor curves.

The calculated volumetric water content was computed from the gravimetric water content for each sample taken at each layer for every water content used. Gravimetric water content is related to volumetric water content as follows:

$$\theta = \omega\left(\frac{\rho_d}{\rho_w}\right) \tag{3-1}$$

where θ, ω, ρ_d, and ρ_w are the volumetric water content, gravimetric water content, dry density and density of water, respectively.

Table 3-1 Testing conditions data for the KRS and HBC.

Soil Type	Loc #	Bulk density (kg/m^3)	Grav Moist (%)	Vol Moist	Degree of Saturation	Matric suction (kPa)
KYS 1	Loc A	1704	7.94	0.1256	0.455	25.1
KYS 2	Loc A	1721	9.39	0.1480	0.639	32.8
KYS 1	Loc B	1740	9.65	0.1535	0.684	17.1
KYS 2	Loc B	1758	10.47	0.1669	0.794	22.6
KYS 1	Loc C	1681	11.07	0.1678	0.801	12.3
KYS 2	Loc C	1708	11.66	0.1787	0.891	15.4
KYS 1	Loc D	1730	12.22	0.1888	0.973	6.1
KYS 2	Loc D	1750	12.28	0.1918	0.998	7.5
HBC 1	Loc E	1999	19.18	0.3223	0.696	109.3
HBC 2	Loc E	2037	21.47	0.3608	0.788	30.12
HBC 3	Loc E	2033	21.25	0.3570	0.779	39.32
HBC 1	Loc F	2055	22.5	0.3782	0.829	15.28
HBC 2	Loc F	2057	22.64	0.3805	0.834	20.50
HBC 3	Loc F	2052	22.32	0.3752	0.822	27.10
HBC 1	Loc G	2064	23.094	0.3880	0.852	17.88
HBC 2	Loc G	2060	22.82	0.3835	0.842	18.48
HBC 3	Loc G	2070	23.43	0.3938	0.866	14.72
HBC 1	Loc H	2065	23.13	0.3887	0.854	16.84
HBC 2	Loc H	2089	24.56	0.4127	0.911	7.30
HBC 3	Loc H	2109	25.76	0.4329	0.959	9.00

Grav Moist = gravimetric moisture content; Vol Moist= volumetric moisture content

3.3 SOIL WATER CHARACTERISTIC CURVE FOR THE KENTUCKY RIVER SAND AND HAMBURG CLAY FROM THE BOX TEST

In the soil water characteristics curve (SWCC), the nonlinear relationship between the degree of saturation and soil suction is the fundamental element used to characterize all aspects of the mechanical properties of unsaturated soils. Several equations were developed for unsaturated soil mechanics' research; this includes Fredland and Zing (1994) and van Genuchten (1980). Among these empirical equations, the van Genuchten (1980) model is the most widely used (W.-H. Zhou et al., 2014) due to its simplicity, which

is used to study the nonlinear relationship between saturation and matric suction. Matric suction refers to the suction component, which relates to the height to which water can be drawn or sucked up (i.e., capillary rise) into unsaturated soil (Eyo et al., 2022). SWCC is typically sigmoidal in shape for a soil and describes the relationship between soil suction and moisture content (Eyo et al., 2022). This research uses the van Genuchten (1980) model to obtain SWCCs. In the box experiment, SWCC curves for two different test soils from the state of Kentucky were used to study the nonlinear relationship between matric suction and volumetric water content by using the van Genuchten model (1980). These soils are identified as the Kentucky River Sand and Hamburg Clay herein. The SWCCs for the soils are shown in Figure 15. The van Genuchten (1980) model is given in Equation 3-2.

$$\theta = \theta_r + \frac{\theta_s - \theta_r}{\left[1 + (\alpha\psi)^n\right]^m}$$ (3-2)

where θ is the volumetric water content; θ_s is the saturated volumetric water content; θ_r is the residual volumetric water content; ψ is the matric suction; α is the curve fitting parameter related to the air entry value, with the version shown in this equation gives the units in kPa; n is related to the water extraction beyond the air-entry value; and m is a function related to the residual matric suction.

As shown in Figures 3-2a and 3-2b, Hamburg clay tends to have a higher volumetric water content and suction values as compared to that of Kentucky River sand. Moreover, Kentucky River Sand data tends to have spread data values, whereas Hamburg Clay has cluster data points. The van Genuchten model tends to perform better with Hamburg clay than Kentucky River sand. VWC refers to the volumetric water content.
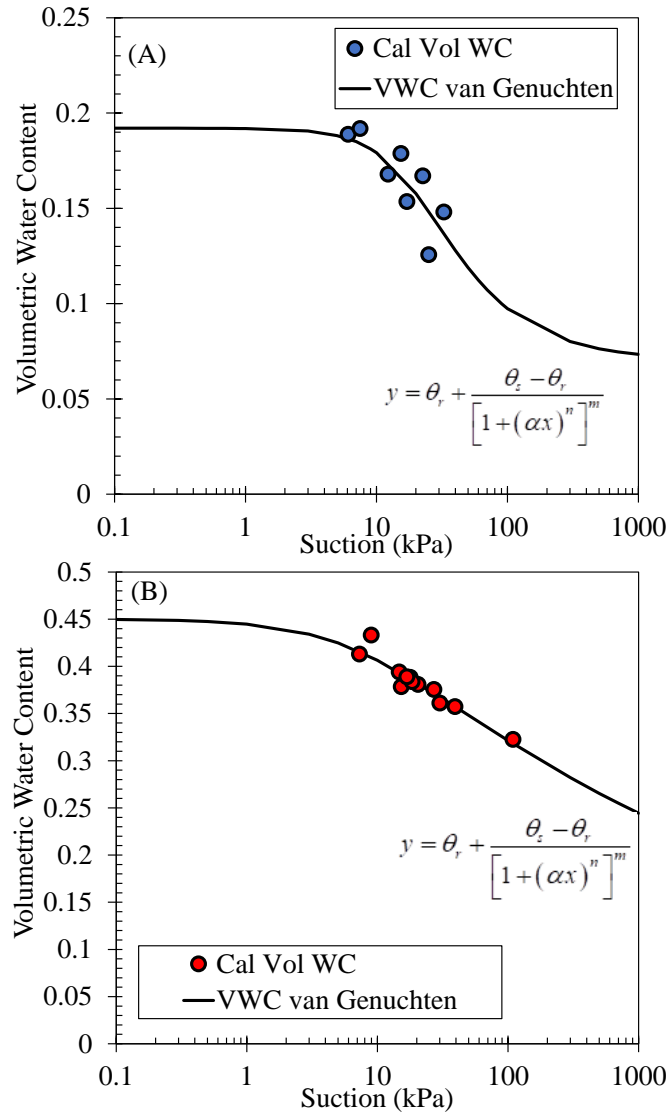
Figure 3-2 Volumetric water content as a function of suction van Genuchten (1980) model. (A) van Genuchten model for the KYS, (B) van Genuchten model for the HBC.

The fitting parameters for the van Genuchten model obtained after optimization Excel Solver are given in Table 3-2.

Table 3-2 Fitting parameters for van Genuchten model.

Fitting Parameters	Kentucky River Sand	Hamburg Clay
α	0.05	0.143
m	1.9	1.135
n	0.48	0.12
θ_s	0.192	0.45
θ_r	0.07	0.03

3.3 CBR MEASUREMENTS IN THE TEST BOX

The DCP testing method is the most common and widely used technique to predict in situ CBR. For the purpose of this research, the DCP index was taken in the soil test box. The DCP test was conducted at each corner of the box using the Vertex Smart DCP equipment, as can be seen in Figure 3-3. More specifically, all data on the DCP index were converted into CBR values using empirical equations reported in the literature. The CBR data presented in ETL 02-19 was developed using the empirical relationship developed by Webster et al. (1992) and is given as follows:

$$\log(CBR) = 2.465 - 1.12\log(DCPI) \tag{3-3}$$

where and DCPI is the penetration resistance or penetration index in units of mm/blow
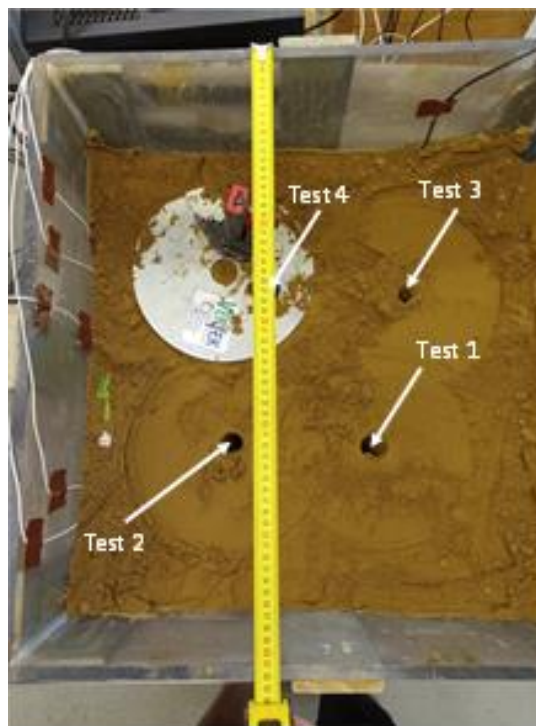
Figure 3-3 Areas where DCP test were performed.

Testing was performed using Kentucky River Sand and Hamburg Clay at four target moisture content levels for each soil type. The gravimetric water content of the Kentucky River Sand was 8, 10, 11, and 12%, whereas that of the Hamburg Clays was 20, 22, 23, and 25%. The sand and the clay were placed in two and three layers, respectively,

and compacted using a 24-kg weight dropped from a height of one foot. Each layer was compacted by dropping the weight of 11 blows per pass for 9 passes per layer.

Figure 3-3 shows the location where CBR test with depth at the four points located at the corners of the box test for the two soil types. The CBR test is used to measure the strength of subgrade for pavement and road design. The CBR is the ratio of the bearing load that penetrates a material to a specific depth compared with the load giving the same penetration into crushed stone (Mendoza and Caicedo, 2019). CBR measures the combination of both stiffness modulus and shear strength (Jenkins and Kerr, 1998). The DCP index was measured at the four corners of the box. The DCP index was then substituted into Equation 3-3 to obtain the CBR at the four locations shown in Figure 3-4.
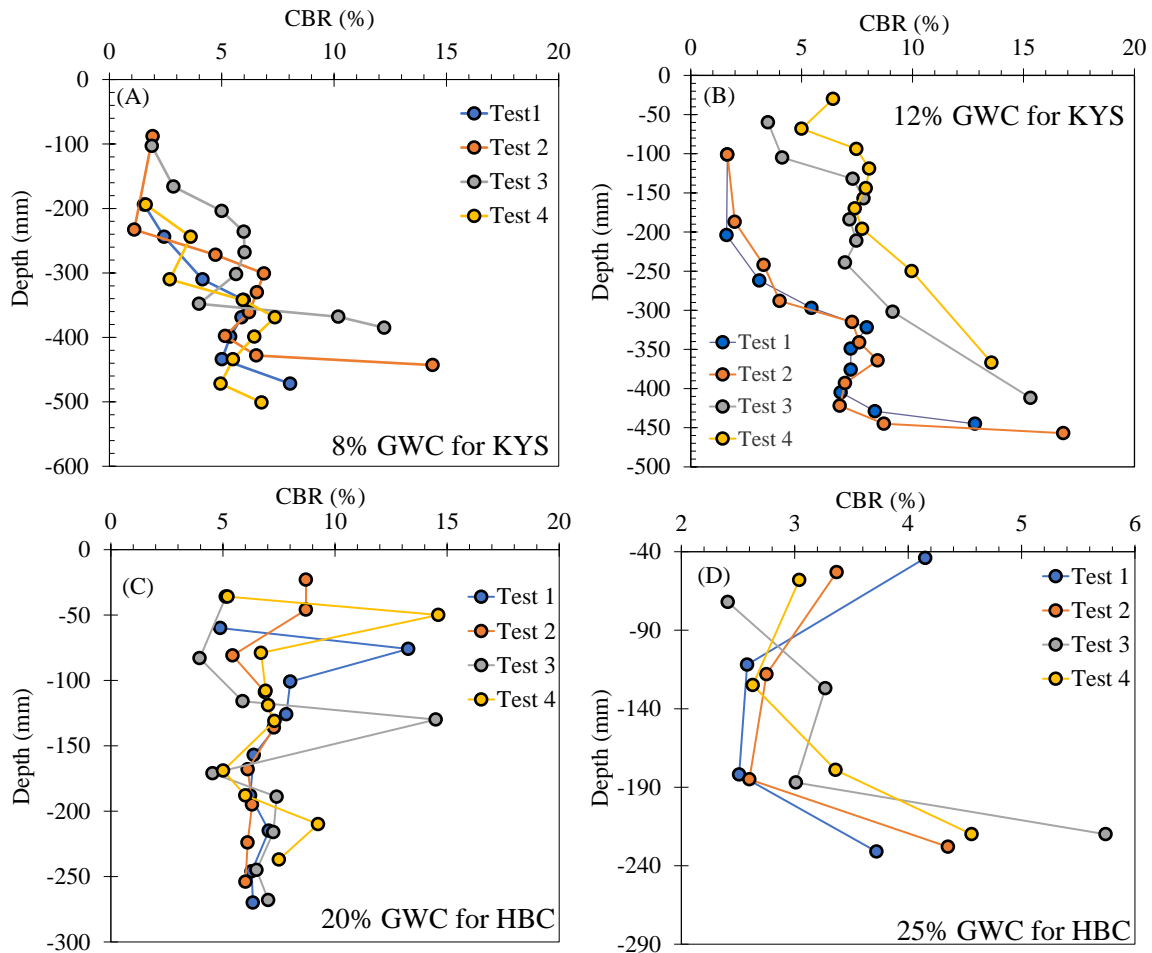
Figure 3-4 CBR variation with depth for KYS and HBC: (A) KYS with the lowest gravimetric water content, (B) KYS with the highest moisture content, (C) HBC with the lowest gravimetric water content, (D) HBC with the highest moisture content.

The minimum and maximum water content data of the CBR were presented in Figure 3-4. The 8% and 12% gravimetric water content are considered for the Kentucky River Sand, whereas the 20% and 25% represent the data from Hamburg CBR. The Kentucky River Sand CBR values range from 2 to 14%, whereas those of the Hamburg Clay range from 4 to 14%, with the Kentucky River data being more clustered than the Hamburg Clay. Table 3-3 shows the data for the average CBR at each test location as a function of water content.

Table 3-3 CBR values with change in gravimetric water content.

CBR	HBC				KYS			
	GWC (%)	Layer 1	Layer 2	Layer 3	GWC (%)	Layer 1	Layer 2	Layer 3
CBR 1	20	7.5	7.8	6.8	8	6.2	5.7	N/A
CBR 2	22	4.2	4.3	4.9	10	8.3	5.7	N/A
CBR 3	23	3.2	2.8	5.1	11	9.6	5.8	N/A
CBR 4	25	3.2	2.9	3.7	12	9.4	9.6	N/A

3.4 SENSORS SET UP FOR THE SEISMIC WAVE VELOCITY AND WATER POTENTIAL MEASUREMENTS

The sensors and accelerometers were placed at each layer for geophysical properties and water potential measurements. We used the moduli value as a standard to compare the DCP, shear wave velocity, and electrical resistivity data. This could help us make small-scale models that show how these seismic waves and electrical measurements change when the unsaturated conditions change. Figure 3-5 shows the set up used for the seismic wave, electrical conductivity (EC), volumetric water content (VWC), and matric suction in the box. For each soil sample, seismic wave velocities were measured including the P wave, and S wave. The electrical conductivity, the matric suction, and the volumetric water content were measured alongside the seismic wave measurement at each layer where sensors and accelerometers were placed.

Electrical conductivity is the measure of the amount of electrical current a material can carry or its ability to carry current whereas the matric suction is the difference between pore air pressure and pore water pressure. Matric suction corresponds to the pressure dry

soil exerts on the surrounding material to equalize the moisture content in the overall block . In isotropic and homogeneous materials, a P-wave travels in a straight line longitudinally. This means that the particles in the solid vibrate along the axis of propagation (the direction of motion) of the wave energy. On the other hand, S-waves are transverse waves, which means that the direction of particle movement of an S-wave is perpendicular to the direction of wave propagation, and the main restoring force comes from shear stress.
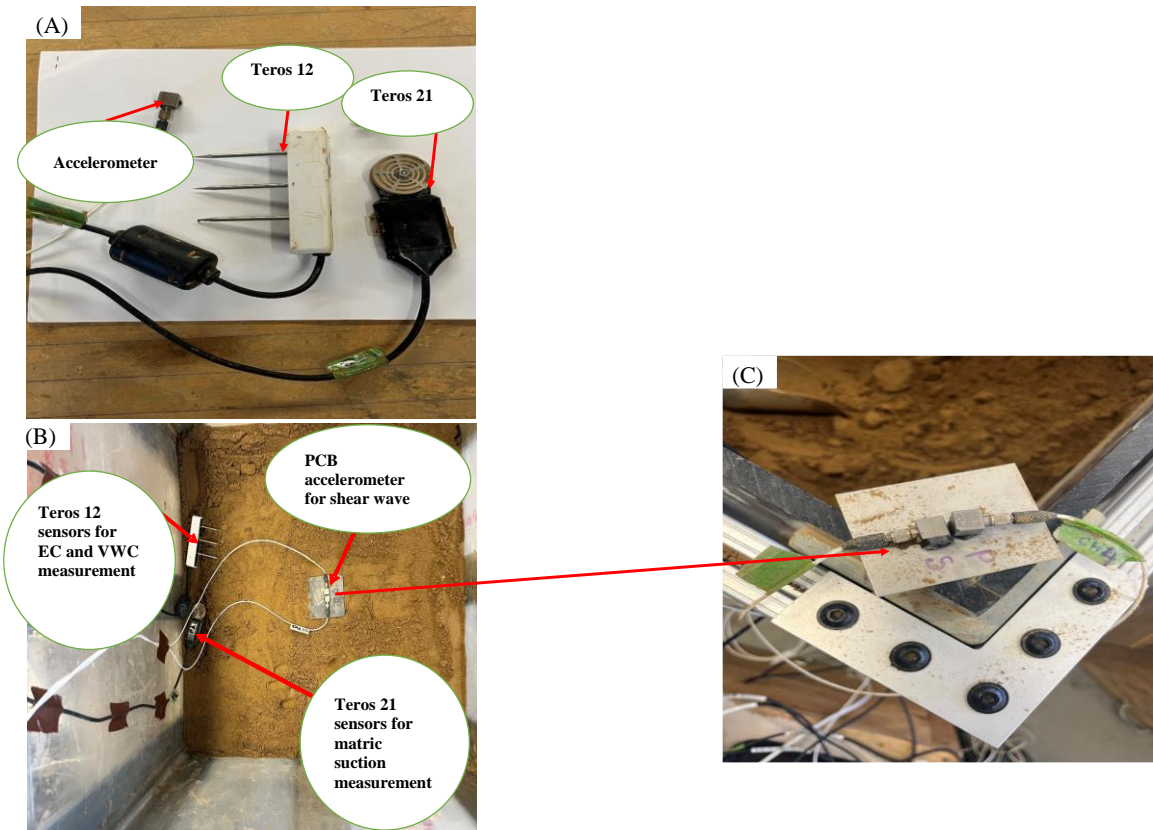
Figure 3-5 Equipment used for seismic wave, electrical conductivity, and water potential measurement.

Table 3-4 Measured geophysical parameters, volumetric water content, and matric suction in the box test.

Soil Type	Meas Vol W C	Layers	Depth (in)	P-wave (m/s)	S-wave (m/s)	EC (mS/cm)	Matric suction (kPa)
KYS	0.141	Layer 1	7	356	198	0.052	25.1
KYS	0.146	Layer 2	14	445	198	0.036	32.8
KYS	0.143	Layer 1	7.2	370	148	0.171	17.1
KYS	0.144	Layer 2	14.6	395	151	0.054	22.6
KYS	0.156	Layer 1	7.4	323	147	0.045	12.3

KYS	0.157	Layer 2	14.7	356	147	0.029	15.4
KYS	0.172	Layer 1	7.6	305	119	0.101	6.1
KYS	0.175	Layer 2	14.9	237	127	0.147	7.5
HBC	0.175	Layer 1	3.5	603	268	0.136	109.3
HBC	0.168	Layer 2	6.5	750	275	0.078	30.12
HBC	0.276	Layer 3	9.5	889	266	0.054	39.32
HBC	0.127	Layer 1	3.7	513	241	0.127	15.28
HBC	0.192	Layer 2	6.7	786	206	0.257	20.50
HBC	0.157	Layer 3	9.7	889	210	0.081	27.10
HBC	0.181	Layer 1	3.8	483	219	0.179	17.88
HBC	0.150	Layer 2	6.7	702	201	0.068	18.48
HBC	0.198	Layer 3	9.6	740	221	0.043	14.72
HBC	0.252	Layer 1	4.0	400	180	0.147	16.84
HBC	0.256	Layer 2	6.8	412	183	0.152	7.30
HBC	0.274	Layer 3	9.7	445	193	0.220	9.00

Seismic wave velocity consisting of the P and S waves were measured at each layer in the soil test box. Accelerometers were placed at two depths in the test box for Kentucky River Sand and three layers for the Hamburg Clay. The P and S waves propagation distance and travel times were measured at each layer with different gravimetric water content in the Box test. The P and S wave were computed using the velocity general relation:

$$V = \frac{d}{t} \tag{3-4}$$

where V in m/s , d and t are the velocity, distance travel by the wave and time of travel in m and s, respectively.

Figure 3-6 shows the Primary waves (P-waves) and Secondary waves (S-waves) propagation and travel times in the two layers in the laboratory box test. Both P and S waves are body waves since they travel through the earth material. the Primary waves (P-waves) are longitudinal compressional waves. As can be presented in Figure 3-6(a)and 3-6(c) P-wave arrive at seismograph stations first because they travel quicker than other waves. Secondary (S-) waves are transverse shear waves. following an earthquake, S-waves arrive at seismograph stations following P-waves and shift the ground perpendicularly as shown in Figure 3-6(b) and 3-6(d).
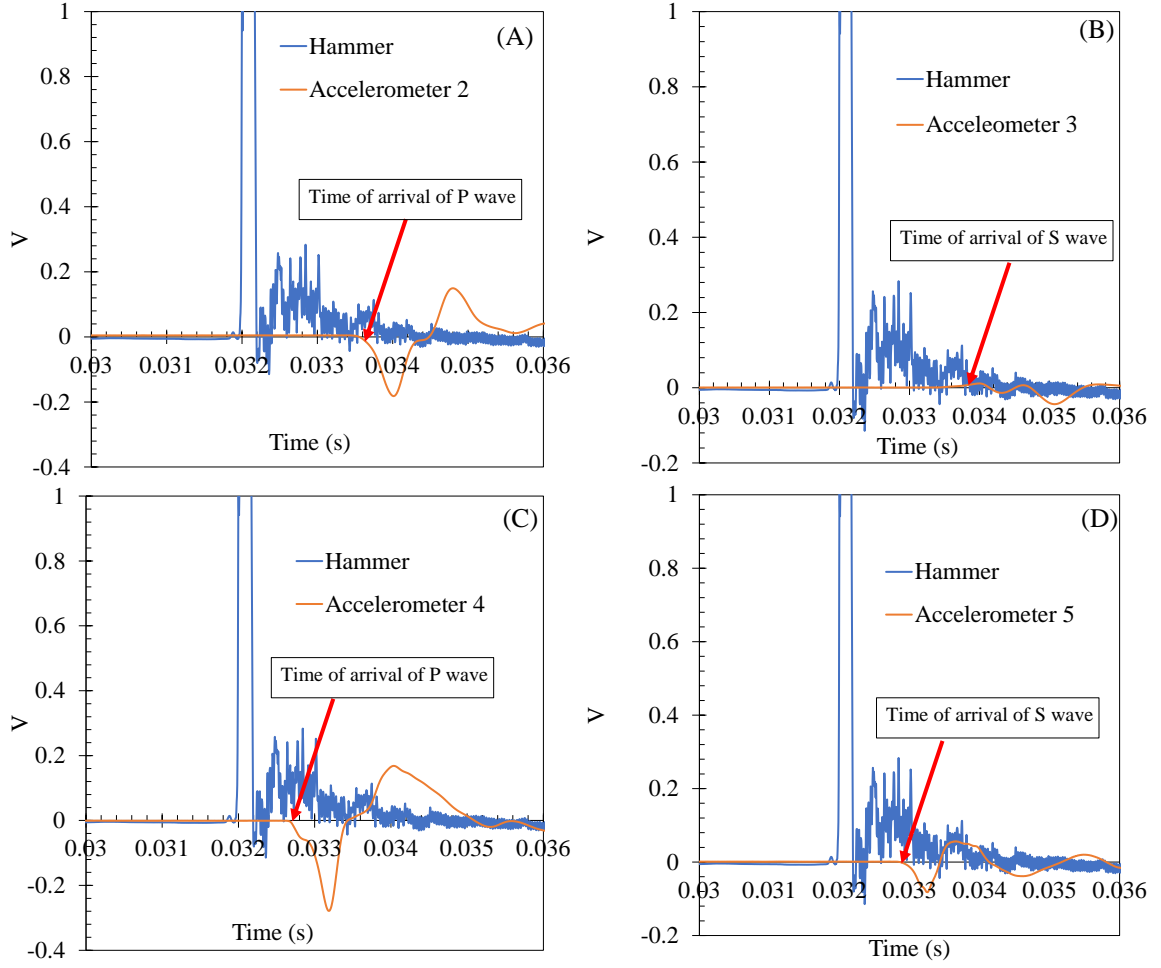
Figure 3-6 A) time of arrival of P wave in Layer 1, (B) time of arrival of S wave in Layer 1, (C) time of arrival of P wave in Layer 2, (A) time of arrival of P wave in Layer 2.

3.5   DATA ANALYSIS

3.5.1   General Elastic Theory

Adama et al., 2023. presented an equation to obtain elastic modulus from the box test of from shear wave velocity, primary wave velocities. This equation is given as,

$$E_{VS} = \rho V_s^2 \, \frac{3\left(\dfrac{V_p}{V_s}\right)^2 - 4}{\left(\dfrac{V_p}{V_s}\right)^2 - 1} \tag{3-5}$$

where V_s, V_p, and ρ are Shear wave velocity, P-wave velocity, and density of soil.

3.5.2   Development of a model of normalized elastic moduli based on electrical conductivity.

A simple regression model cannot adequately describe the data. It is noted that van Genuchten (1980) presented a sigmoidal function to describe the variation of the effective degree of saturation as a function of the matric suction. We believe that this model will fit our data because elastic modulus and electrical conductivity are both functions of volumetric moisture content and matric suction, and both parameters are described by van Genuchten model. Therefore, the relationship between elastic modulus and electrical conductivity can be best described using van Genuchten sigmoidal model which involves both parameters. The basic form of the van Genuchten (1980) model is given as

$$y = \left[\left(1 + a \cdot x \right)^b \right]^{-c}$$
(3-6)

where a, b, and c are optimization-found fitting parameters that describe a sigmoidal function that starts at unity (i.e., 1.0) and varies to 0. The a-parameter roughly describes the point of maximum curvature at the beginning of the sigmoid. The b-parameter describes the inflection point of the curve, and the c-parameter roughly describes the end point of the sigmoidal function. Using the van Genuchten (1980) model on the test data in Figure 3-7 to show how it changed, a new function was made to show how the normalized elastic modulus changed when electrical conductivity changed. The new model is given as,

$$\frac{E_{VS}}{E_{VSAT}} = \left[\left(1 + a \cdot EC \right)^b \right]^{-c}$$
(3-7)

where a, b, and c are fitting parameters for the proposed model for the test. EC is the electrical conductivity; E_{VSAT} is the elastic modulus at nearly saturated conditions. In Equation 3-7, the a-parameter describes the point of maximum curvature; the b-parameter describes the inflection point; and the c-parameter describes the point of the sigmoidal shape. Because the modulus elasticity is normalized with the modulus at near saturated

46

conditions, the normalized parameter yields 1.0 at saturated conditions. For this study, the a, b, and c-parameters were found by optimization using the Excel Solver function. Microsoft Excel Equation Solver was used to minimize the least square difference between measured and predicted values to establish fitting parameters.

The fitting parameters vary greatly based on the original input data and optimization boundary conditions. The optimization used all the measured data from the sensor measurements. Figure 3-7 presents a basic analysis of the elastic modulus as a function of electrical conductivity. In this figure, the elastic modulus data are plotted as a function of the measured electrical conductivity. The elastic modulus values were normalized by a reference value, which is defined as the modulus of elasticity at nearly saturated conditions, and the value was set to 173 MPa and 65 MPa for Hamburg Clay and Kentucky River Sand, respectively. The sole purpose of the reference modulus was to scale the elastic modulus and make the resulting parameter dimensionless. These fitting parameters for the proposed model for test soil Equation 3-7 are given in Table 3-5

Table 3-5 Fitting parameters for the proposed model for the test soil.

Fitting Parameters	Kentucky River Sand	Hamburg Clay
a	10.5	11
b	-1.25	-1.5
c	-0.7	-0.8

Figure 3-7(a) shows the normalized elastic modulus obtained from shear wave velocity as a function of electrical conductivity for Kentucky River Sand while Figure 3-7(b) shows the normalized electrical modulus obtained from shear wave velocity as a function of elastic conductivity for Hamburg Clay. Table 3-6 shows how these mechanical properties and elastic modulus are based on the effective degree of saturation. The elastic modulus from Table 3-6 was derived by using Equation 3-7. The effective degree of saturation of 1.0 implies saturated conditions and the modulus value for Kentucky River Sand nearest an effective degree of saturation of 1.0 was 65 MPa and for Hamburg Clay was 173 MPa. For the modulus values derived from DCP data, the saturated modulus for Kentucky River Sand was approximately 15, and for Hamburg Clay the saturated modulus was roughly 41 MPa.

Table 3-6 Mechanical properties and the conditions based on moisture content.

Soil Type	e	Layers	Depth (in)	n	Se	G (MPa)	E_{Vs} (MPa)	E_{DCP} (MPa)	E_{Vs} / E_{VSAT}
KYS	0.68	Layer 1	7	0.40	0.455	61.58	157.26	11.29	2.41
KYS	0.68	Layer 2	14	0.41	0.639	61.37	169.01	10.71	2.59
KYS	0.67	Layer 1	7.2	0.40	0.684	34.84	97.85	13.59	1.50
KYS	0.66	Layer 2	14.6	0.40	0.794	36.13	102.23	10.73	1.57
KYS	0.75	Layer 1	7.4	0.43	0.801	32.68	89.53	14.92	1.37
KYS	0.73	Layer 2	14.7	0.42	0.891	34.15	95.12	10.80	1.46
KYS	0.72	Layer 1	7.6	0.42	0.973	21.83	61.57	14.82	0.94
KYS	0.70	Layer 2	14.9	0.41	0.998	25.14	65.29	14.99	1.00
HBC	0.58	Layer 1	3.5	0.37	0.696	120.47	331.76	64.01	1.92
HBC	0.58	Layer 2	6.5	0.37	0.788	126.82	360.76	65.74	2.09
HBC	0.58	Layer 3	9.5	0.37	0.779	118.64	344.24	60.19	1.99
HBC	0.58	Layer 1	3.7	0.37	0.829	97.43	264.71	43.79	1.53
HBC	0.58	Layer 2	6.7	0.37	0.834	71.18	208.28	45.01	1.20
HBC	0.58	Layer 3	9.7	0.37	0.822	73.98	217.57	48.67	1.26
HBC	0.58	Layer 1	3.8	0.37	0.852	80.42	220.45	37.37	1.27
HBC	0.58	Layer 2	6.7	0.37	0.842	67.76	197.24	34.08	1.14
HBC	0.58	Layer 3	9.6	0.37	0.866	81.91	237.70	49.86	1.37
HBC	0.58	Layer 1	4.0	0.37	0.854	54.34	149.22	37.37	0.86
HBC	0.58	Layer 2	6.8	0.37	0.911	56.16	154.69	34.78	0.89
HBC	0.58	Layer 3	9.7	0.37	0.959	62.47	172.93	40.88	1.00

As shown in Figure 3-7, Hamburg Clay data tends to have a higher conductivity value as compared to Kentucky River Sand. This is because of the conduciveness of clay

(Qi and Wu, 2022) and its higher moisture content since water is a good conducting material as well (Guan et al., 2022). The conductivity of the Kentucky River sand varied between 0.029 and 0.171 mS/cm. Moreover, Kentucky River Sand data tended to cluster and show relatively minor conductivity variations with the elastic modulus derived from DCP tended to cluster and show relatively minor electrical conductivity variations with changing the elastic moduli from the range of 0.02 to 0.06 mS/cm. The data is spread out more in the range of 0.06 to 0.16 mS/cm, with the DCP-derived modulus being higher than the shear wave velocity's elastic modulus with variation in electrical conductivity. The conductivity of Hamburg clay varied between 0.043 and 0.257 mS/cm. In the Hamburg Clay data, the values are more scattered and consistent. As shown in Figures 3-7(a) and 3-7(b), the proposed model performed better in low-conductivity soil and higher-strength soil. Stiff soil tends to have smaller pore volumes because, because it has a small pore volume, it tends not to be conductive. Therefore, the proposed model performs better for stiff soil with low conductivity because of the resisting condition of stiff soil.

The DCP index data from the box test was averaged within a particular layer and converted into CBR using Equation 3-8. For this research, the CBR values were then converted into elastic modulus values using the empirical equation presented by Powell et al. (1984). The Powell et al. (1984) equation was modified herein as,

$$E_{DCP}(MPa) = C_1 17.6(CBR)^{0.64} \qquad (3\text{-}8)$$

where $= C_1$ is a calibration factor to account for variations in testing conditions, such as variations due to depth (i.e., increased lateral restraint), soil types, moisture content, and stress state. The calibration factor was determined for this present study by comparing the modulus values obtained from the DCP to the modulus values obtained directly from the shear wave velocities obtained from the box test because they both describe mechanical behavior of soil. The calibration factors for Equation 3-8 are given in Table 3-7.

Table 3-7 Calibration factors.

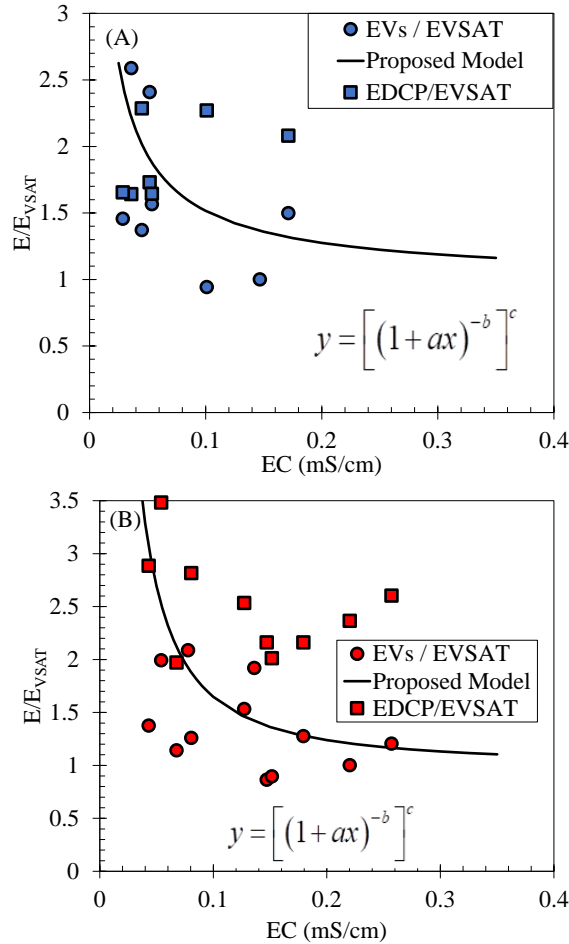| calibration factor	Kentucky River Sand	Hamburg Clay
C_1	1.6	5.2

Figure 3-7 Normalized elastic modulus as a function of electrical conductivity: (A) Normalized Elastic moduli with EC for the KYS, (B) Normalized Elastic moduli with EC for the HBC.

3.5.3 Sensitivity analysis of the fitting parameters for Hamburg Clay

In Figure 3-8 (a), the original data point is approximately E=90 MPa. We observed that as the percentage change increases, the initial point decreases. Specifically, the starting points for percentage changes of +100%, +50%, -10%, and -20% correspond to E values of 45, 60, 100, and 110, respectively. In Figure 3-8 (a), the data changes before reaching the inflection point within the range of 0.02 to 0.1 mS/cm in electrical conductivity. Additionally, within this range, the difference between the original data and the percentage change data increases with higher percentage changes. The data converges to an E value of about 17.24 MPa, which corresponds to E under saturated conditions. This figure demonstrates that data with a higher percentage increment is below the original data, while

data with a smaller percentage change is consistently above the original data throughout the analysis.

In Figures 3-8(b), the initial data point is approximately E=90 MPa. The figure also illustrates that the starting point is higher with a higher percentage change. Specifically, the starting points at +100% and +50% correspond to E=100 MPa, while the starting points at -10% and 20% correspond to E=80 and 70 MPa, respectively. Additionally, the figure shows an intersection point for all data at EC=0.1 mS/cm and E=30 MPa. Prior to the intersection point, data with a higher percentage increment is positioned above the original data, while those with a smaller percentage change are below the original data. After the intersection point, their behavior is reversed. Similar to Figure 3-8(b), all data converges to values close to E at a saturated point.

In Figures 3-8(c), the starting point of the original data is E=100 MPa. The saturation point of data with higher percentages is greater than those with a smaller percentage change. As with the previous figures, the data points converge to E at a saturated point. A sensitivity analysis was performed based on the fitting parameters. All three fitting parameters were increased by 50 % to observe the change in each parameter as compared to the proposed model. As can be observed in Figures 21b, 21c, and 21d the variation of, there is a big variation in a range of 0.04 to 0.12 mS/cm whereas a minor variation with greater conductivity for all three cases. The sensitivity analysis captures the small variation that was observed during the box test.
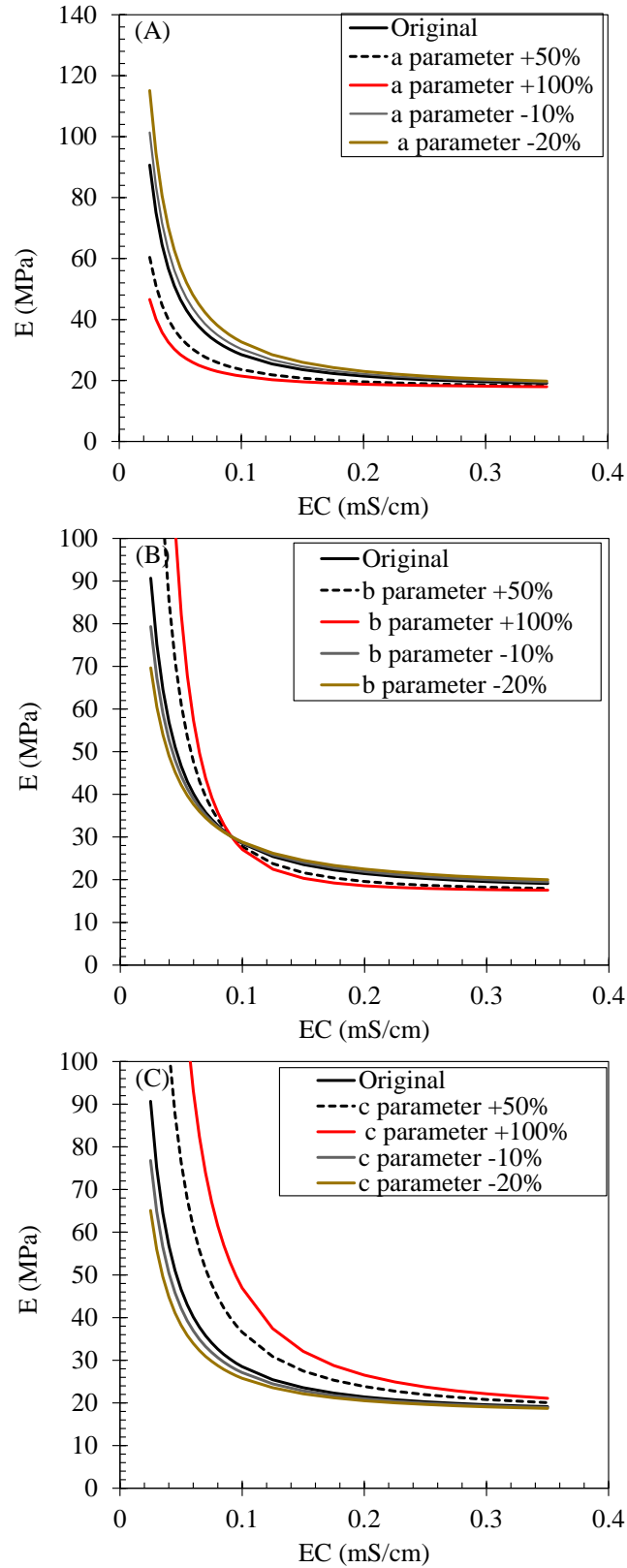
Figure 3-8 Elastic modulus as a function of electrical conductivity: (A) Sensitivity analysis with a parameter; (C) sensitivity analysis with b parameter; (D) sensitivity analysis with c parameter.

3.6   APPLICATION OF THE PROPOSED MODEL TO THE FIELD

3.6.1   General Description of the Rouen field site

This research outlines a plan to utilize data obtained from extensive laboratory testing to establish fundamental geophysical-geotechnical correlations. Simultaneously, researchers at the M2C Lab, University of Rouen Normandy, France, are investigating the research site located at the CEREMA Centre for Research on Risks, the Environment, Mobility, and Urban Planning in Rouen, France. The primary objective of the research is to link field DCP measurements with electrical, electromagnetic, and seismic geophysical data. Additional support for these initiatives comes from the establishment of both large-scale test sites, where some locations were compacted at specific CBR strengths. Figure 3-9 shows both sectional and plan views of the research site in France. The testing location is divided into three distinct areas—Area 1 (A1), Area 2 (A2), and Area 3 (A3)—each consisting of three layers of compacted soil, each 250 mm thick and approximately 7 m wide. These areas are separated into four-meter-wide "dead zones, "named for their lack of reliable data. The site dimensions are relative to the origin in the northwest corner of the test site, as shown in Figure 3-9(b), with the cartesian coordinate system assuming the Y-direction is directly east, and the X-direction is directly south. The beginning and finishing points of areas A1, A2, and A3 are at 0 meters, 11.3 meters, and 22.3 meters, respectively, with dimensions of 6.8, 17.8, and 28.8 meters.
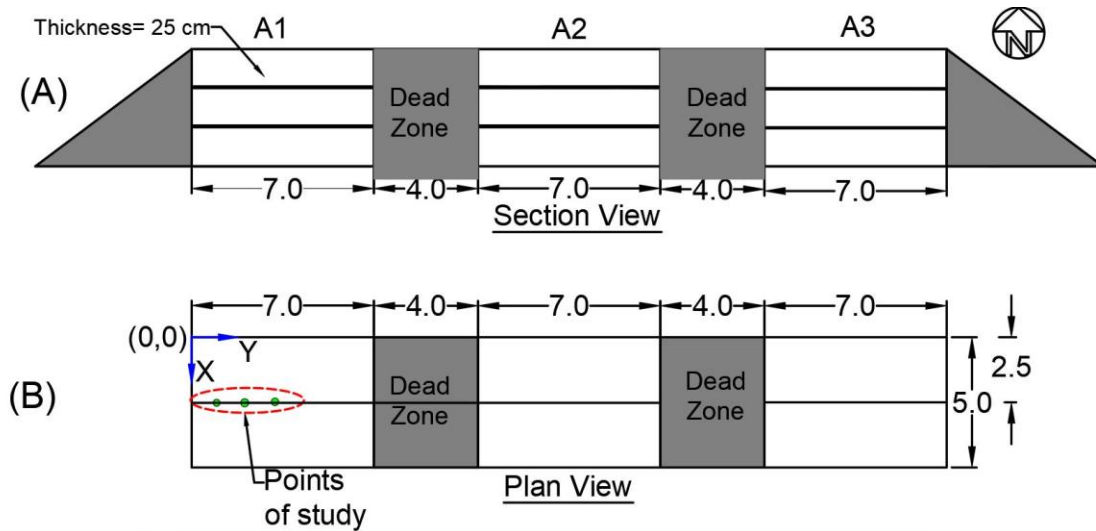

Figure 3-9 Test site. (A) the depth of investigation of the three areas, (B) Plan (i.e., arial) view of the three areas of investigation. All dimensions given in the figure are in units of meters (Adama et al., 2023).

3.6.2   Measured field data at characteristic locations.

The variations of electrical conductivity, shear wave velocity-based modulus, and CBR-based elastic modulus data with depth are shown in Figure 3-10. Three points of study were chosen along the centerline of the test site in the X-direction (i.e., X = 2.5 m). The three study points were selected at positions Y = 1.3 m, 1.8 m, and 3.8 m. The data obtained from the first 20 cm of the MASW results were unreliable because of the errors associated with the dispersion curve fitting for the highest frequencies. At Area 1, the natural ground was located at around 65 cm. Figure 3-10(f) depicts the variation of CBR calculated modulus as a function of depth. For this study, the CBR values were converted into elastic modulus values using the empirical equation presented by Powell et al. (1984). The Powell et al. (1984) equation was modified herein as,

$$E(MPa) = C_1 \times 17.6(CBR)^{0.64} \tag{3-9}$$

where C_1 is a calibration factor to account for variations in testing conditions, such as variations due to depth (i.e., increased lateral restraint), soil types, moisture content, and stress state. As will be discussed in subsequent sections, the calibration factor was determined for this present study by comparing the modulus values obtained from Equation 3-10 to the modulus values obtained directly from field geophysics data. For this study the calibration factor, C_1 equaled approximately 1.0. Figure 3-10(a) shows the variation of electrical resistivity with depth at the three different points ranging from 36 Ω.m to 65 Ω.m.

The electrical resistivity increased with depth at point Y= 1.3m, roughly the same rate of increase. but decreased with depth at locations Y= 1.8 m from ground surface to a depth of 0.45 m and increased from this depth to the natural ground level. The electrical resistivity increases with depth at location Y=3.8 at from the ground level to a depth of 0.16 m and at depth 0.65 m to the natural ground level but it decreases in between these depths. Figure 3-10(b) shows electrical conductivity variations with depth. The electrical resistivity values are constant throughout the depth of investigation. This similarity is indicative of the uniformity of the test material at the three points of study. The relationship between electrical conductivity and resistivity is quite simple: they are inversely proportional to each other. This means that as the conductivity of a material increases, its

resistivity decreases, and vice versa. Mathematically, this relationship can be expressed as $EC = 1/ER$, where EC is electrical conductivity in mS/cm and ER is electrical resistivity in Ω.m. This equation shows that when the resistivity of a material is known, its conductivity can be easily calculated, and vice versa.

Figure 3-10(c) shows the shear wave velocity varied between 117 m/s to 180 m/s. The shear wave velocity trends strongly with the DCP data. The shear wave velocity initially increased from the ground surface to a depth of approximately 0.15 m and afterwards decreased from a depth of 0.15 m to 0.38 m. The decrease in shear wave velocity between 0.3 m and 0.4 m somewhat confirms the DCP data showing a soft zone was in the second layer of Area A1. As was discussed previously, this similarity is indicative of the uniformity of the test material at the three points of study. It is speculated that the rate of increase and decrease is most likely reflective of the variation in water content with depth, at the time of testing. Figure 3-10(d) shows the variation of elastic modulus obtained directly by using shear wave velocity as a function of depth. (Adama et al., 2023). presented an equation to obtain field modulus of elasticity from shear wave velocity. This equation is given as,

$$\frac{E}{E_{ref}} = \beta \left(\frac{V_s}{V_{ref}} \right)^2 \tag{3-10}$$

where β is a term that describes the influence of the mass density and the Poisson's ratio on the changes in the modulus of elasticity. The elastic modulus values are normalized by a reference elastic modulus, E_{ref} set to 100 MPa. The sole purpose of the reference modulus is to scale the measured modulus values and make the resulting parameter dimensionless. The shear wave velocity values have also been normalized with a reference shear wave velocity, V_{sref}. For this study, $V_{sref} = 150$ m/s, which was arbitrarily chosen as a typical value for loose to medium dense sands (Hardin and Richart, 1963).
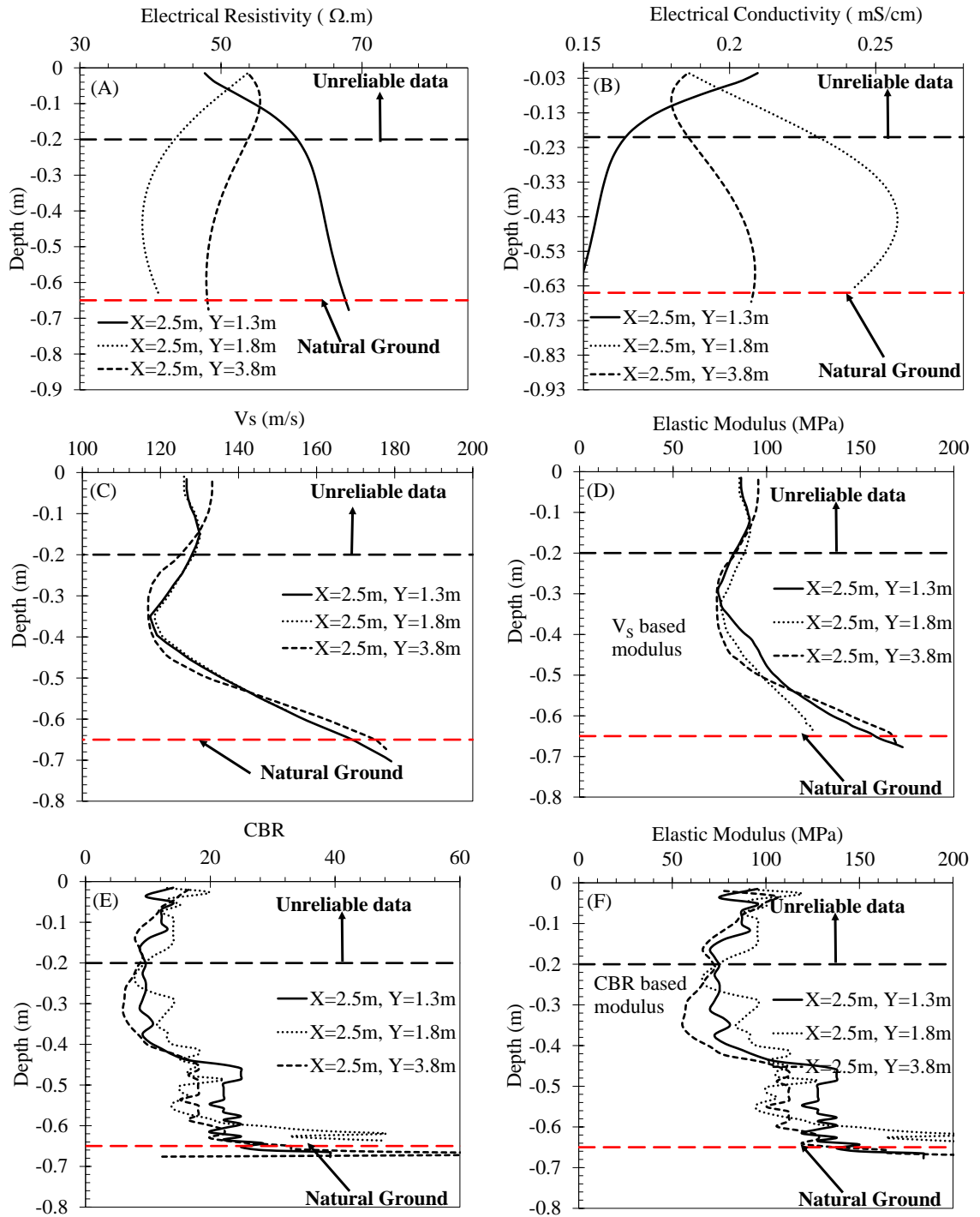
Figure 3-10 Geophysical and geotechnical data variation with depth at Area A1. (A) Electrical conductivity variation with depth, (B) Elastic modulus-based shear wave velocity variation with depth and (D) elastic modulus based on CBR variation with depth.

3.6.3   Performance of proposed model under field conditions

The elastic modulus value was used as a common variable for comparing the DCP, shear wave velocity, and electrical conductivity in this research. More specifically, all three data points were converted to elastic modulus values using empirical equations reported in the literature or using empirical equations developed for this research. The elastic modulus based on the shear wave velocity and DCP were obtained from Equations 3-9 and 3-10, respectively. The elastic modulus value was used as a common variable for comparing the DCP, shear wave velocity, and electrical conductivity in this research. More specifically, all three data points were converted to elastic modulus values using empirical equations reported in the literature or using empirical equations developed for this research.

The box test was performed to ascertain a relationship between the electrical conductivity and the elastic modulus values. The proposed model from the box test relating electrical conductivity and elastic modulus based on shear wave velocity was applied on the French site to evaluate the performance of the model. The fitting parameters for both soil types from the box test were applied to the French site, and the findings show a better performance with the Kentucky River Sand parameters than that of Hamburg Clay. As shown in Figure 24, the electrical data is not varying. The lack of variation in electrical measurements reflects the lack of variation in moisture content at the site and not the variation in mechanical behavior.

Thus, further studies will be required to correlate geophysical electrical data to mechanical behavior, which includes functions that couple hydrologic changes with mechanical behavior changes. The preliminary assessment of this observation is that the electrical data was only able to capture the slight variation of the moisture content with depth at the test site and not the variations in the mechanical behavior. Thus, it is recommended that future efforts to relate geophysical electrical methods to mechanical behavior incorporate functions that couple changes in the hydrologic regime with changes in mechanical behavior. The findings of these studies show that elastic modulus values obtained using shear wave velocity measurements strongly trend with elastic modulus derived using DCP. Consequently, this study shows that geophysical techniques, specifically shear wave velocity measures, can be used to directly obtain the elastic

modulus without using CBR. The nearly saturated elastic modulus used was 65 MPa. The fitting parameters used in the site is the average fitting parameters of the sand and Clays since the site presented a mixture of these two soil types. The sensitivity analysis performed in the box test only captures small variations but fails to account for the larger variations observed in the field. The initial attempt to adjust the box test to reflect the changes in the field was not adequate. Since the box test only captures a narrow range of variation, further experiments are needed to account for the smaller variations observed in the field.". The Box test captures variation within a very small range therefore more experiments to smaller variation in the field.

Table 3-8 Fitting parameters applied on the French site in Rouen.

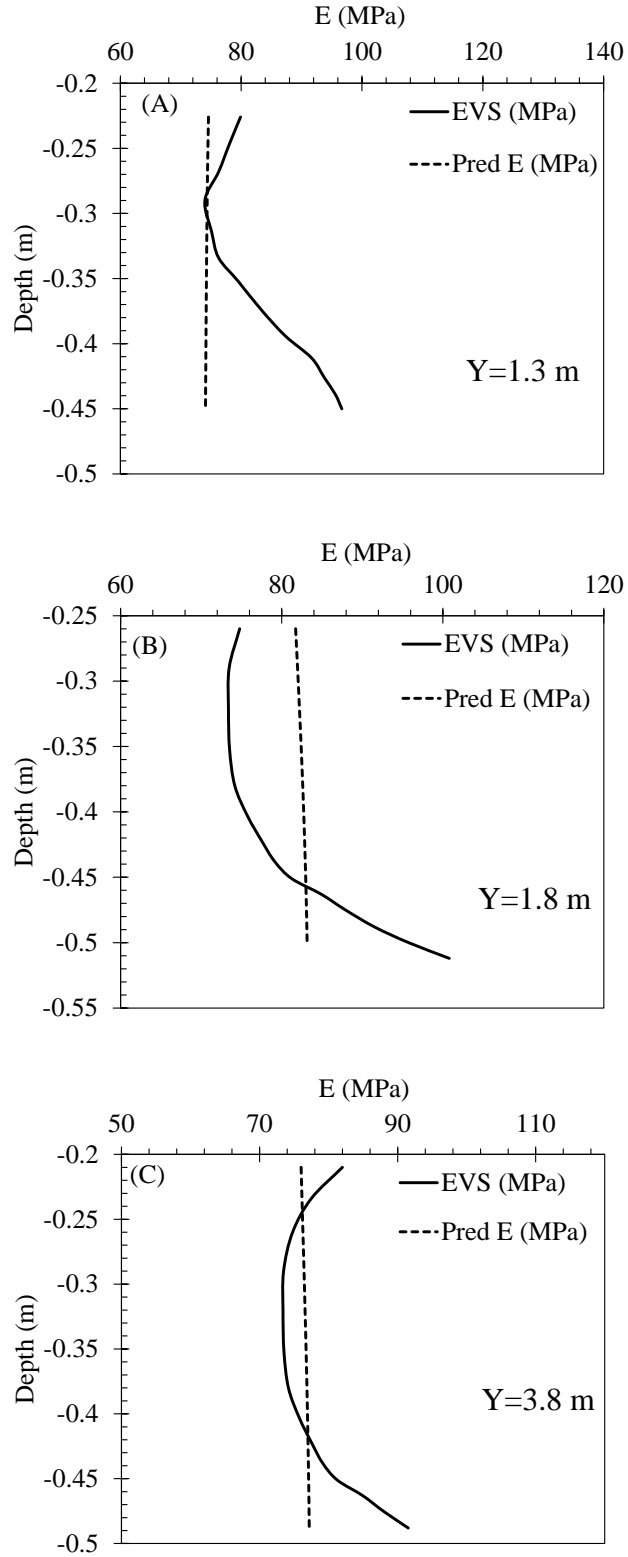| Fitting Parameters	Average of KYS and HBC
a	10.5
b	-1.25
c	-0.7

Figure 3-11 Elastic modulus based on Electrical conductivity, and shear wave velocity and its variation with depth. (A) at 1.3 m, (B) at 1.8 m and (C) at 3.8 m.

CHAPTER 4. SUMMARY AND CONCLUSIONS

The research discussed the development of a methodology to evaluate the feasibility of a possible airport based on CBR and elastic modulus values generated from shear wave velocity and electrical resistivity. The elastic modulus was calculated directly from shear wave velocity using concepts of elastic theory and wave propagation in an elastic material. An equation was developed based on an analysis of elastic modulus and shear wave velocity data collected from triaxial testing using bender elements. The general equation implicitly accounts for confinement and bulk mass density. Therefore, only direct observations of shear wave velocities are required to establish a straightforward connection. Electrical resistivity data was analyzed in relation to CBR data in unpublished research where electrical measurements were taken continually during CBR tests.

The CBR-electrical resistivity expressions yield an equation to estimate the CBR value based on the original soil conditions using electrical resistivity data. The CBR and elastic modulus values derived from geophysics were used to compute factors for assessing airfield suitability, such as the gross maximum weight and the maximum number of aircraft passes. This method offers more efficient and direct spatial coverage of suitability assessment criteria compared to discrete data received via DCP measurements at several places. A comparison study was conducted to analyze variations in comparable CBR values with respect to depth and along a profile. The results indicated that the shear wave velocity-derived CBR data closely aligned with the DCP-derived data.

The CBR values obtained from electrical resistivity did not correspond with the other two CBR values. Considering the moisture conditions at the test site, it was suggested that the CBR values generated from electrical resistivity probably simply indicated changes in moisture content. Implementing the proposed process flow for assessing the suitability of a potential airfield demonstrated that spatial shear wave velocity derived CBR data could differentiate between areas in the Rouen, France, test site that met or exceeded the assessment criteria and areas that did not meet the criteria.

While the example focused on one type of aircraft, it is possible to apply the same process flow to other types of aircraft. The studies' findings indicate that CBR values acquired by shear wave velocity measurements align with CBR values obtained through

DCP. This study demonstrates that geophysical approaches, particularly shear wave velocity estimates, can effectively evaluate field suitability as well as or even better than the existing method. This research also discusses the relationship between seismic wave velocity and DCP-derived elastic modulus based on electrical conductivity to ascertain soil stiffness. The study compared elastic modulus values derived from DCP penetration resistance with those acquired from shear wave velocity values and the elastic modulus from the suggested model based on the box test. The study utilized a sigmoidal model to examine the relationship between soil stiffness and electrical conductivity in unsaturated conditions.

The study's findings indicate that elastic modulus values derived from shear wave velocity and DCP measurements are more effective in low conductivity and high stiffness conditions. The elastic modulus in the box test was determined by directly calculating it from the measured shear wave velocity using elastic theory and wave propagation in elastic materials. Accelerometers were utilized at each layer of the test boxes to assess data on elastic modulus and shear wave velocity in order to formulate a comprehensive equation. The modulus of elasticity (E) and California Bearing Ratio (CBR) are associated based on soil sample elastic properties. The equation by Powel et al. (1984) suggests a connection between E and CBR. Subgrade modulus can be determined by utilizing California Bearing Ratio (CBR) values and Dynamic Cone Penetrometer (DCP) values.

The study compared elastic modulus values calculated from DCP penetration resistance to corresponding elastic values calculated from shear wave velocity measurements. This method offers a more efficient and direct spatial coverage of suitability assessment criteria compared to discrete data received via DCP measurements at several places. A sigmoidal model, inspired by van Genuchten (1980), was created to depict the elastic moduli in relation to electrical conductivity due to the limitations of a basic regression model. The suggested model showed improved performance in denser, less conductive soil. The investigations demonstrate a significant correlation between elastic modulus values obtained by shear wave velocity measurements and those estimated using DCP. This study demonstrates that geophysical approaches, particularly shear wave velocity estimates, can be utilized to directly calculate stiffness in the field, but the electrical data does not align well with these results.
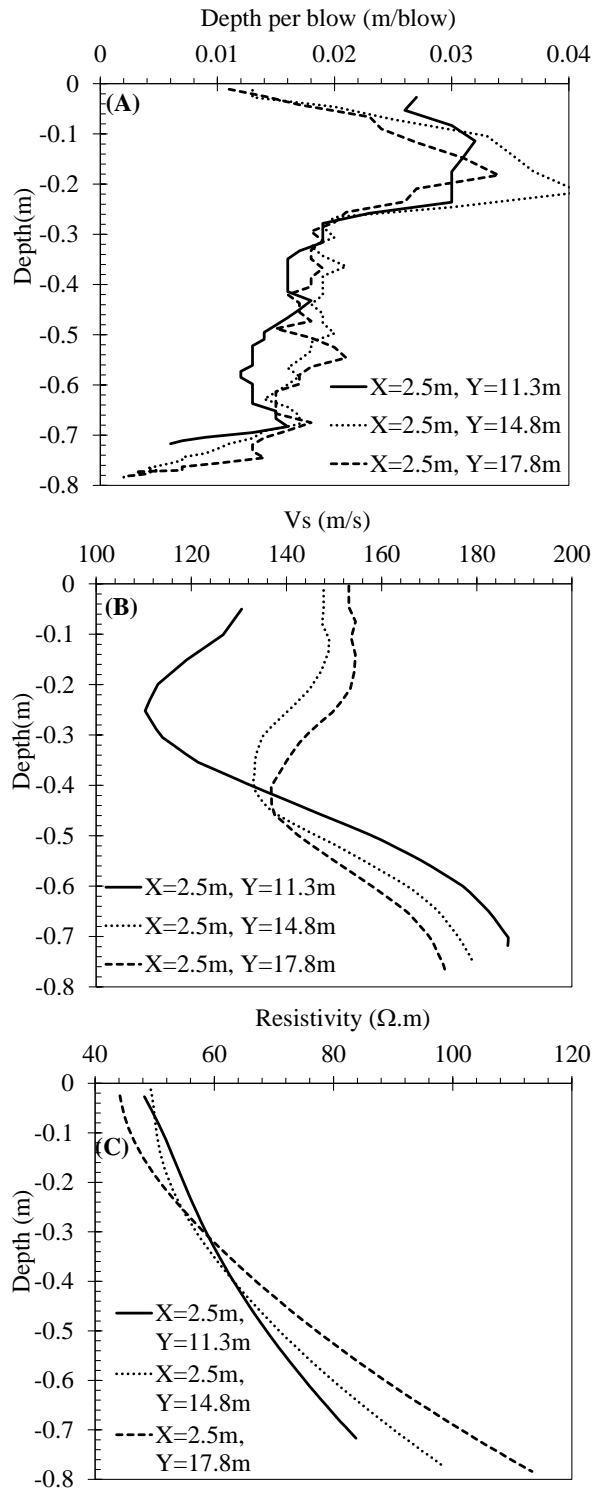
APPENDICES

Figure A-1 Geophysical and geotechnical data variation with depth at Area A2. (A) DCP
variation with depth, (B) shear wave velocity variation with depth and (C) electrical resistivity
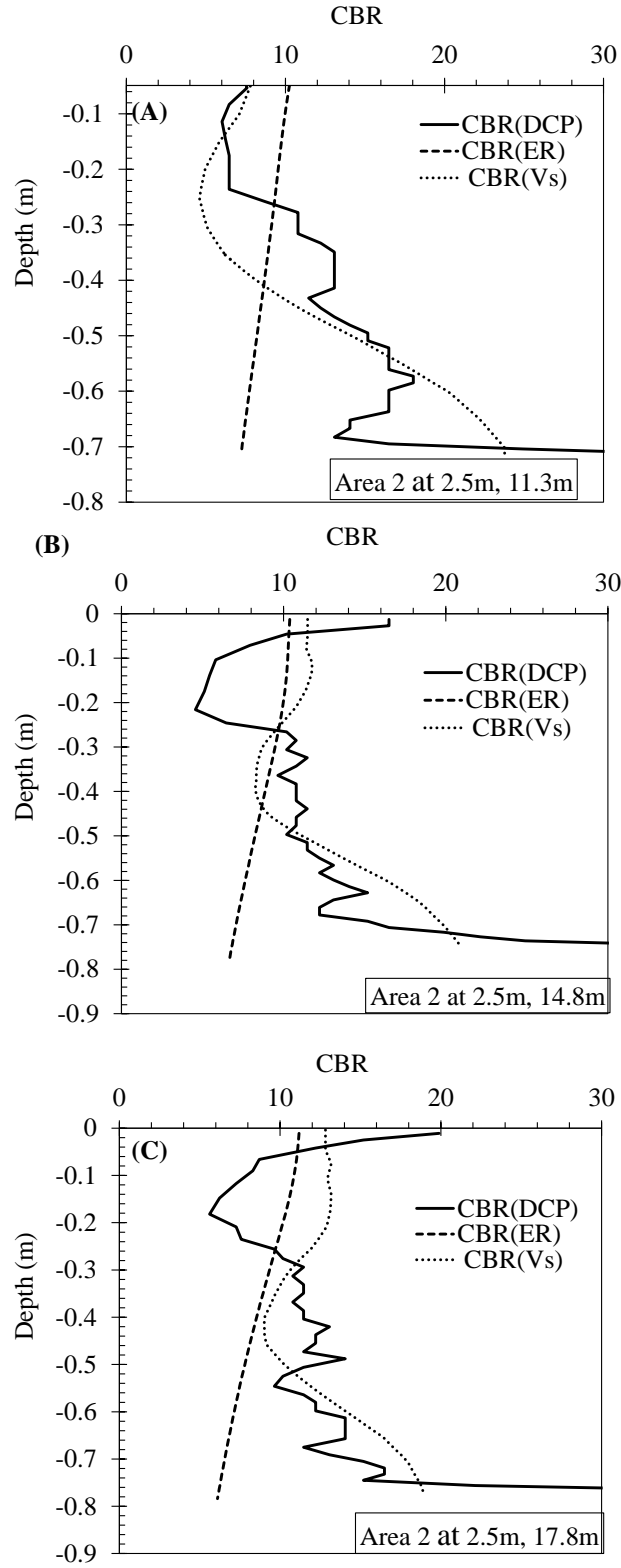variation with depth.

Figure A-2 CBR based on ERT, DCP, and shear wave velocity and its variation with depth. (A) at 11.3 m, (B) at 14.8 m and (C) at 17.8 m.
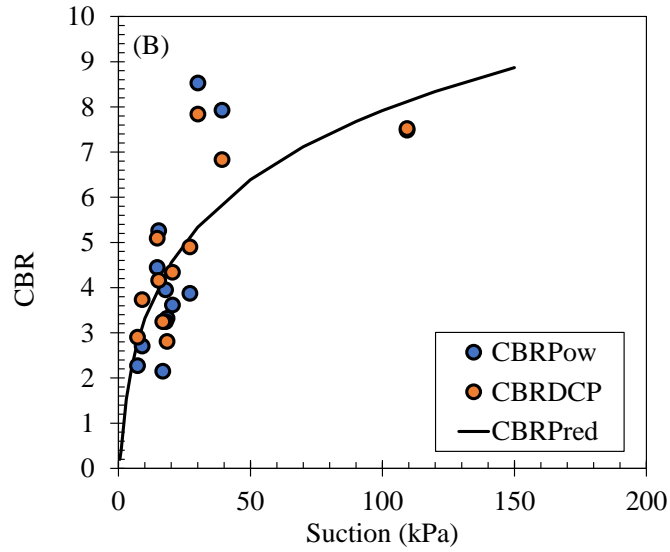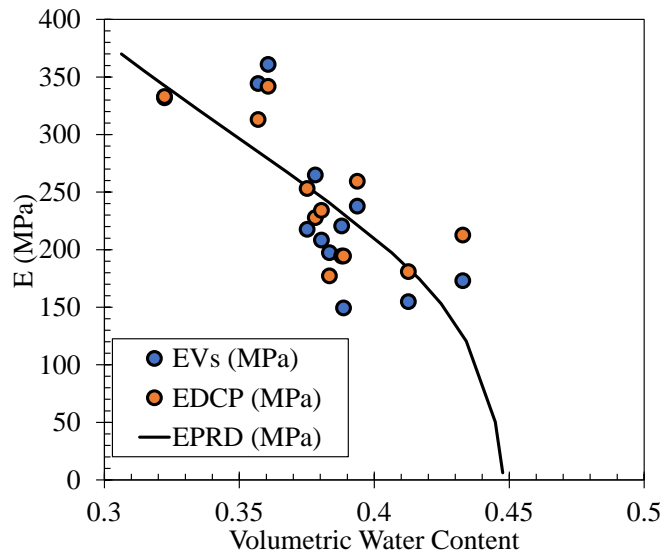
Figure B-1 CBR as a function of suction.

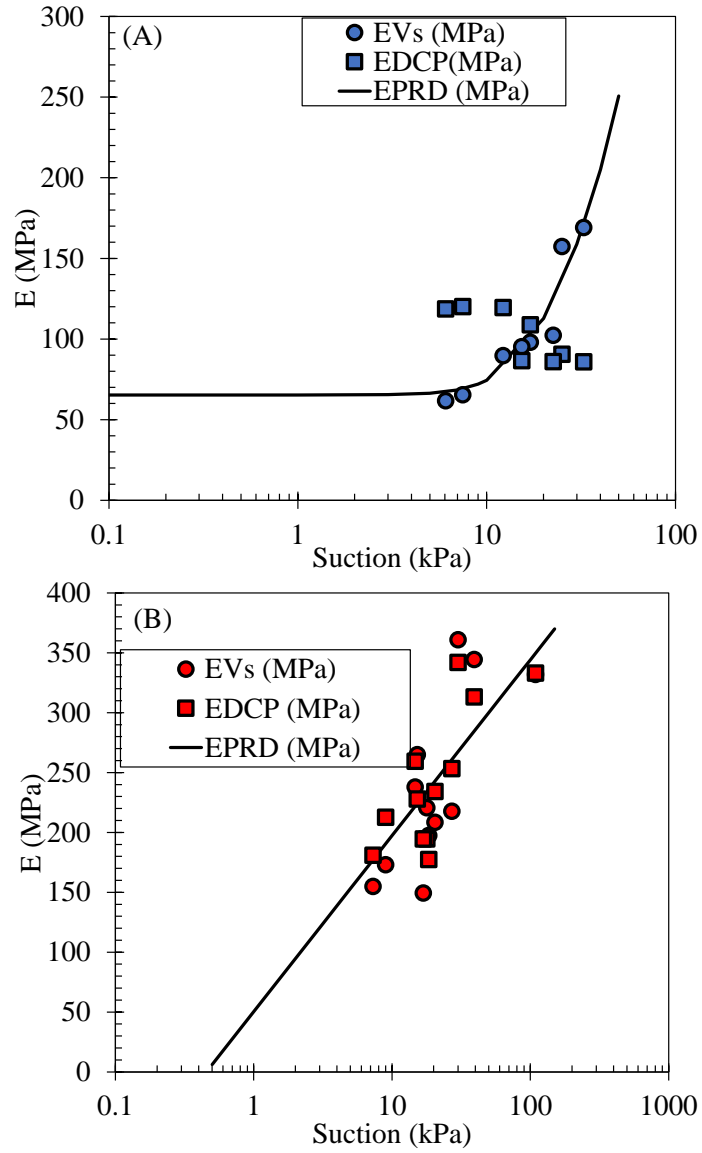Figure B-2 Elastic modulus as a function of volumetric water content.

Figure B-3 Elastic modulus as a function of suction by Archie law: (A) for Kentucky River Sand, (B) for Hamburg Clay.
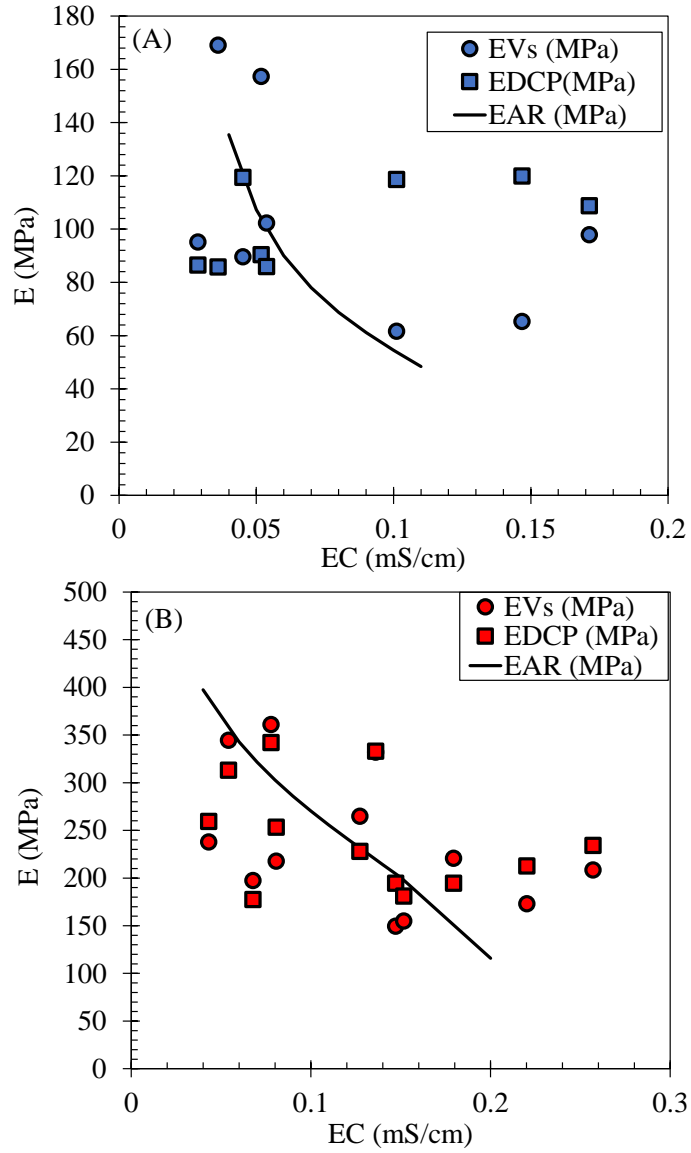
Figure B-4 Elastic modulus as a function of electrical conductivity by Archie law: (A) for Kentucky River Sand, (B) for Hamburg Clay.
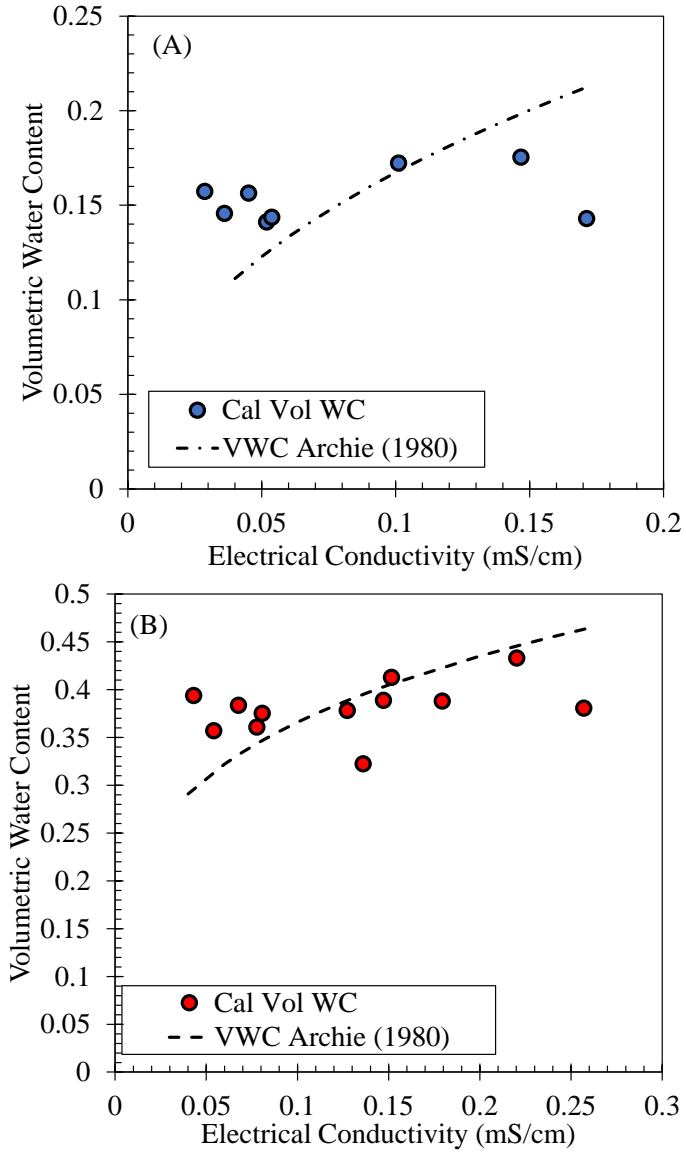
Figure B-5 Volumetric water content as a function of electrical conductivity by Archie law: (A) for Kentucky River Sand, (B) for Hamburg Clay.

REFERENCES

Abd, I. A., Fattah, M. Y., and Mekkiyah, H. (2020). Relationship between the matric suction and the shear strength in unsaturated soil. Case Studies in Construction Materials, 13, e00441.

Adama, D., Bryson, L. S., and Wang, A. (2023). Airfield suitability assessment from geophysical methods. Transportation Geotechnics, 42, 101059.

Adebisi, N. O., Ariyo, S. O., and Sotikare, P. B. (2016). Electrical resistivity and geotechnical assessment of subgrade soils in southwestern part of Nigeria. Journal of African Earth Sciences, 119, 256–263.

Bery, A. A. (2016). Slope monitoring study using soil mechanics properties and 4-D electrical resistivity tomography methods. Soil Mechanics and Foundation Engineering, 53(1), 24–29.

Bryson, L. S., and Sayre, C. A. (2021). Using shear wave velocity for general airfield pavement design. Symposium on the Application of Geophysics to Engineering and Environmental Problems, Nashville, TN, 14-19 March 2021. https://doi.org/10.4133/sageep.33-040.

Carvalho, J., Torres, L., Castro, R., Dias R., Mendes-Victor, L. (2009). "Seismic velocities and geotechnical data applied to the soil microzoning of western Algarve, Portugal." Journal of Applied Geophysics, 68(2), 249–258.

Cheng, G. Y., Liu, X. J., and Qiu, R. (2011). Study on the Correlation between Strength Parameters and Shear Wave Velocity of Pavement Subgrade Soil. Applied Mechanics and Materials, 90, 2002–2007.

Crawford, M. M., and Bryson, L. S. (2018). Assessment of active landslides using field electrical measurements. Engineering Geology, 233, 146–159.

Davich, P., Labuz, J. F., Guzina, B., and Drescher, A. (2004). "Small strain and resilient modulus testing of granular soils., Report No. 2004-39, Final Report, Minnesota Department of Transportation, St. Paul, Minnesota.

Foti, S., Lai, C. G. and Lancellotta, R. (2002). "Porosity of fluid saturated porous media from measured seismic wave velocities." Geotechnique, 52(5), 359-373.

Hardin, B.O., Richart, F. (1963). "Elastic wave velocities in granular soils." Journal of the Soil Mechanics and Foundations Division, ASCE, 89(SM1), 33–65.

Hurley, M. A. (2021). Geophysical Techniques Used for the Analysis and Prediction of Soil Strength and Mechanical Behavior.

Jenkins, P., and Kerr, I. A. (1998). The strength of well graded cohesive fills. Ground Engineering, 31(3).

Juarez, M. B., Mondelli, G., and Giacheti, H. L. (2023). An overview of in situ testing and geophysical methods to investigate municipal solid waste landfills. Environmental Science and Pollution Research, 30(9), 24779–24789.

Kang, M., and Lee, J.-S. (2015). Evaluation of the freezing–thawing effect in sand–silt mixtures using elastic waves and electrical resistivity. Cold Regions Science and Technology, 113, 1–11.

Kang, M., Qamhia, I. I., Tutumluer, E., Hong, W.-T., Doyle, J. D., Carr, H. T., Hodo, W. D., Cox, B. C., and Tingle, J. S. (2022). Bender element field sensors for base course stiffness measurements in airport pavements. In Advances in Transportation Geotechnics IV (pp. 861–876). Springer.

Kim, S. Y., Hong, W.-T., and Lee, J.-S. (2019). Role of the coefficient of uniformity on the California bearing ratio, penetration resistance, and small strain stiffness of coarse arctic soils. Cold Regions Science and Technology, 160, 230–241.

Lee, J.-S., and Yoon, H.-K. (2015). Theoretical relationship between elastic wave velocity and electrical resistivity. Journal of Applied Geophysics, 116, 51–61.

Mayne, P. W., and Rix, G. J. (1995). Correlations between shear wave velocity and cone tip resistance in natural clays. Soils and Foundations, 35(2), 107–110.

Mendoza, C., and Caicedo, B. (2019). Elastoplastic framework of relationships between CBR and Young's modulus for fine grained materials. Transportation Geotechnics, 21, 100280.

Mendoza, C., and Caicedo, B. (2019). Elastoplastic framework of relationships between CBR and Young's modulus for fine grained materials. Transportation Geotechnics, 21, 100280.

Mukabi, J. N. (2016). Review of DCP Based CBR-UCS and resilient modulus models for applications in highway and airport pavement design. US Army, 10, 1.

Muttashar, W. R., and Bryson, L. S. (2020). Constitutive model for predicting stress-strain behavior of fine-grained sediments using shear-wave velocity. Marine Georesources and Geotechnology, 38(8), 896–910.

Narzary, B. K., and Ahamad, K. U. (2018). Estimating elastic modulus of California bearing ratio test sample using finite element model. Construction and Building Materials, 175, 601–609.

Powell, W.D., Potter, J.F., Mayhew, H.C., and Nunn, M.E. (1984). "The structural design of bituminous roads." TRRL Laboratory Report 1132, Transport and Road Research Laboratory, Department of Transport, Crowthorne, Berkshire, 62 pp.

Rahardjo, H., Melinda, F., Leong, E. C., and Rezaur, R. B. (2011). Stiffness of a compacted residual soil. Engineering Geology, 120(1–4), 60–67.

Raheem, A. M. (2023). Developing a New Soil-Water Characteristic Model Using Nondestructive Electrical Properties for Unsaturated Soil. Geotechnical and Geological Engineering, 41(2), 1589–1601.

Santamarina, J. C. and Aloufi, M. A. (1999). "Small Strain Stiffness: A Micromechanical Experimental Study." In Proceedings of Pre-failure Deformation Characteristics of Geomaterials, IST99, vol. 1, pp. 451-458.

Santamarina, J., Klein, A., Fam, M.A. (2001). Soils and Waves: Particulate Materials Behavior, Characterization and Process Monitoring, J. Wiley and Sons, New York.

Shao, H., Zhang, J., Fan, T., and Li, Z. (2015). Electrical method to evaluate elastic modulus of early age concrete. Construction and Building Materials, 101, 661–666.

Sheriff, R. E. (2002). "Encyclopedic dictionary of applied geophysics: SEG Geophysical Reference Series No. 13," 4th Ed., Society of Exploration Geophysicists (SEG), Tulsa, Oklahoma, 429 pp.

Sheriff, R. E., and Geldart, L. P. (1995). Exploration seismology. Cambridge University Press, Cambridge.

Tatham, R.H. (1982). "Vp/Vs and lithology." Geophysics, 47(3), 336-344.

Wang, H., Hu, C.-H., Hsieh, C.-H., Hsieh, S.-H., Arany, G., Hickey, C., Hoover, R. A., Higgins, T., Kissinger, B., and Mundell, J. (2016). Transportation and Infrastructure Geophysics. Symposium on the Application of Geophysics to Engineering and Environmental Problems 2015, 484–492.

Webster S. L., Grau R. H. and Williams T. P., 1992, "Description and Application of Dual Mass Dynamic Cone Penetrometer," Instruction Report, GL-92-3, Army Engineers Waterways Experiment Station, Vicksburg, Miss.

Zhou, M., Wang, J., Cai, L., Fan, Y., and Zheng, Z. (2015). Laboratory investigations on factors affecting soil electrical resistivity and the measurement. IEEE Transactions on Industry Applications, 51(6), 5358–5365.

VITA

Dabo Adama

Education

Master of Science: 2021 – Present, Civil Engineering, University of Kentucky

Lexington, Kentucky

Bachelor of Science: 2018, Geological Engineering, Kwame Nkrumah University of
Science and Technology

Kumasi, Ghana

Experience:

Research and Teaching Assistant: 2021-2023, University of Kentucky

Lexington, Kentucky, USA

Intern Engineer: 2018 Summer, Building Roads, and Research Institute (BRRI)

Kumasi, Ghana

Intern Engineer: 2023 Anderson Professional Service.

Lexington, Kentucky, USA

Publication: Adama, D., Bryson, L. S., and Wang, A. (2023). Airfield suitability
assessment from geophysical methods. Transportation Geotechnics, 42, 101059.